TÉCNICO LISBOA

Development of a recovery mass for trapping arsenic containing compounds from hydrocarbon feeds

Martim André Norte de Carvalho Anastácio

Thesis to obtain the Master of Science Degree in

Chemical Engineering

Supervisor(s):

Dr. Michel Thomas

Dr. Francisco Lemos

Examination Committee

Chairperson: Prof. Sebastião Alves

Supervisor: Dr. Francisco Lemos

Members of the Committee: Prof. Maria Filipa Ribeiro

November 2016

This page was intentionally left blank

“Le savant n’est pas l’homme qui fournit les vraies réponses, c’est celui qui pose les vraies questions. “

- Claude Lévi-Strauss -

This page was intentionally left blank

Acknowledgements

First of all, I want to express a word of gratitude to all the structure of IFP Energies nouvelles for the excellent reception that provided me, and the Instituto Superior Técnico to maintain this partnership and enable the realization of this internship.

I thank Luis for all of your help since the first day that we arrived.

I am very grateful to my supervisors at IFP Energies nouvelles, Michel Thomas and Antoine Hugon, for their dedication, support and precious advises provided throughout this internship. It was a pleasure to work with both. I also thank Michel for all car rides in the days of strike. To professor Francisco Lemos, thanks for the suggestions that you gave me, for your availability and interest in my work.

I would also to thank everyone in Catalysis and Separation department for the receiving welcome, rapid integration and for all the affection during my time at IFPEN; especially I want to thank Anthony Tanguy for the precious help in the laboratory, for the great friendship, patience, for all the portuguese words that we changed and for the car ride to the airport. I also want to thank Sandra Montpeyroux for teach me how to use the reactor and Florence Del Toso by the work time provided to explain me the operation of the sulphurization unit.

To my IFPEN collegues who made easier these 6 months and help me to integrate, Kenza, Marine, Tiffany, Fabien (thanks for our tennis games), Antoine, Louis, Ester, Mafalda, Leonor, Ana Rita, Alberto, Marisa, Pedro, thank you all.

To my Portuguese friends, Mariana, Bárbara e Tiago, this amazing time would have been so great without all of you.

To my friends who stayed in Portugal or in another corner of the world, a huge thank you for everything, specially: Miguel Costa, Fábio Santos, João Marcos, Guilherme Carvalho, Guilherme Jerónimo, João Fiúza, Miguel Agapito, Pedro Barreto, Manuel Vilela and Nuno Cortesão.

I would also like to thank my family, Joaquim, my mother and my grandmother for all your efforts and encouragements. Without you nothing of this could be possible.

This page was intentionally left blank

Resumo

Este trabalho teve como objetivo estudar a eficiência de sólidos para sequestrar compostos orgânicos de arsénio. Como tal, foram aplicados métodos de preparação de catalisadores, nomeadamente impregnação seca usando diferentes percursores metálicos e tratamentos térmicos (calcinação). Todos os catalisadores preparados foram caracterizados por Adsorção-dessorção de Azoto, Porosimetria de Mercúrio, Difracção Raios-X e Fluorescência Raios-X a fim de determinar as propriedades texturais e os teores em metal. Para ativar os catalisadores foi realizada sulfuração.

Foram efectuados testes catalíticos num reactor Grignard a 250˚C e 35 bar de pressão de hidrogénio, utilizando duas alimentações concentradas em compostos orgânicos de arsénio de diferentes naturezas: trietilarsina e trifenilarsina. A captura mássica destas alimentações aumenta com a dispersão do metal no catalisador. Em geral, as conversões são duas vezes superiores para $AsPh_3$ e o Níquel é o precursor metálico mais eficiente para capturar ambos os compostos, demonstrando conversões de 47% para $AsEt_3$ e 100% para $AsPh_3$ e constantes cinéticas de 4.0×10^{-3} min^{-1} e 1.3×10^{-1} min^{-1}, respetivamente. Mesmo para outros metais, com baixas concentrações de arsénio (215.5 ppm) na forma de $AsPh_3$ as conversões são de 100% mas as velocidade de captura são maiores para o Níquel (k = 1.3×10^{-1} min^{-1}) seguido pelo Cobalto (k = 6.4×10^{-2} min^{-1}) e Ferro (k = 5.3×10^{-4} min^{-1}). Catalisadores que contêm molibdénio na sua composição demonstram maiores conversões para elevadas concentrações de arsénio (2155 ppm), aumentando esta conversão em 3 vezes.

Foram realizados testes com uma alimentação concentrada em arsénio e enxofre, provando que a conversão para o arsénio é maior do que para o enxofre, 100% e 75% respetivamente, com uma seletividade em arsénio de 6.4.

Palavras-chave: captura de arsénio; trietilarsina; trifenilarsina; catalisadores metálicos; constantes cinéticas; seletividade

This page was intentionally left blank

Abstract

The aim of this work was to study the solids efficiency to trap organo-arsenic compounds. For that purpose, catalyst preparation methods were applied, by dry impregnation using different metal precursors and thermal treatments (calcination). All prepared catalysts were characterized by Nitrogen Adsorption-desorption, Mercury Porosimetry, X-Ray Diffraction and X-Ray Fluorescence in order to determine textural properties and metal contents. To activate the catalysts, sulphurization was done.

Standard and reproducible catalytic tests were performed in a Grignard reactor at 250°C and 35 bar of hydrogen pressure, using two different natures of organo-arsenic concentrated feeds: triethylarsine and triphenylarsine. The mass trapping of this feeds increases with the dispersion of the metal on the catalyst. In general, the conversions are 2 times higher for $AsPh_3$ and Nickel is the most efficient metal precursor to trap both feeds, presenting conversions of 47% for $AsEt_3$ and 100% for $AsPh_3$ and kinetic constants of 4.0×10^{-3} min^{-1} and 1.3×10^{-1} min^{-1}, respectively. Even for other metals, with low concentrations of arsenic (215.5 ppm) in form of $AsPh_3$ the conversions are 100% but the trapping rate are higher for nickel ($k = 1.3\times10^{-1}$ min^{-1}) followed by cobalt ($k = 6.4\times10^{-2}$ min^{-1}) and iron ($k = 5.3\times10^{-4}$ min^{-1}). Catalysts that have molybdenum in their composition demonstrate higher conversions for high concentrations of arsenic (2155 ppm), increasing this conversion 3 times.

Tests with a concentrated feed of arsenic and sulphur were performed, proving that the conversion for arsenic is higher than for sulphur, 100% and 75% respectively, with a selectivity for arsenic of 6.4.

Key words: arsenic trapping; triethylarsine; triphenylarsine; metallic catalysts; kinetic constants; selectivity

This page was intentionally left blank

Table of Contents

List of Figures

List of Tables

This page was intentionally left blank

List of Abbreviations

RON – Research Octane Number

MON – Motor Octane Number

FCC – Fluid Catalytic Cracking

HDS – Hydrodesulphurization

VGO – Vacuum Gasoil

LPG – Light Petroleum Gas

LCO – Light Cycle Oil

HCO – Heavy Cycle Oil

TAPV – Total Accessible Pore Volume

R – Ratio; Rate

WHSV – Weight Hourly Space Velocity

PD – Packing Density

XRD – X-Ray Diffraction

XRF – X-Ray Fluorescence

FWHM – Full-Width Half-Maximum

$AsPh_3$ – Triphenylarsine

$AsEt_3$ – Triethylarsine

$AsMet_3$ – Trimethylarsine

3-Me-Thi – 3-methylthiophene

bp – Boiling Point

GC – Gas Chromatography

AAS – Activated Alumina Support

This page was intentionally left blank

1 Context and Objectives

The evolution of refineries is related to the petroleum products demand, in other words, this evolution has been driven by market trends but also by improving the quality of products (increase of RON for gasoline and cetane number for diesel). Currently, the demand for light products and middle distillates increases instead of the demand for heavy products which is decreasing. Another important parameter is environmental regulation that determines the quality upgrading of petroleum products.

The FCC gasoline produced has a very high octane number, especially for paraffinic and naphthenic loads, but must be desulphurized without reduction of RON. This desulphurization is carried out by HDS units, which use bimetallic catalysts, in the oxide form, of Mo/W and Co/Ni. To activate the catalyst is necessary to sulfurize these metal oxides.

Unfortunately, arsenic compounds, present in some feeds at trace levels, are responsible for poisoning, reducing the catalyst activity due to the formation of intermetallic phases. However, there are only few information about the deactivation of HDS catalysts by arsenic.

The aim of this work is to develop a recovery mass, composed by transition metals deposited on a support such as alumina, which can eliminate such organo-arsenic compounds from the feeds to be treated. The main objectives are:

- Develop a methodology for the catalytic tests:
    - Using 2 referenced catalysts (RC1 and RC2);
    - Using 2 arsenic compounds ($AsEt_3$ and $AsPh_3$) with different concentrations;
    - Evaluate the reproducibility of the tests.
- Synthetize trapping mass catalysts:
    - Perform preparation and activation methods such as dry impregnation, calcination and sulphurization;
    - Discover the importance of use the dispersion agent in the impregnated solutions.
- Evaluate the performance of the catalysts:
    - Working with the simple model feed, define the best metal/metals responsible for trapping organo-arsenic compounds;
    - Discover the kinetics of organo-arsenic adsorption;
    - Test the competition between dearsenification with desulphurization.

This page was intentionally left blank

2 State of Art

2.1 What is Fluid Catalytic Cracking?

Catalytic cracking process was developed in 1920 by Eugene Houdry. Houdry process was based on cyclic fixed bed configuration. There has been continuous upgrades in catalytic cracking process from its incept of fixed bed technology to latter fluidized bed catalytic cracking (FCC) [1].

For the production of gasoline, FCC (Fluid Catalytic Cracking) is the most suitable due to its orientation towards to produce light olefins, responsible for a high octane number.

Octane number is a measure of the ability of fuel to resist to auto-ignition during the compression phase (knocking). To determine the octane number of a given gasoline there are two standard reference fuels, isooctane (has an octane number of 100 due to its knocking resistance) and heptane (which causes knocking and has an octane number of 0), that are compared with the amount of knocking which fuel causes when combusted. The result of octane number is defined as the volumetric percentage of isooctane required in a mixture with heptane to correspond the knocking behavior of the fuel being tested.

In fact, two standard procedures are used namely Research Octane Number (RON) and Motor Octane Number (MON), depending on the operating conditions and type of engine. Normally, the octane number present on the pumps at service stations is the RON value or the average octane value between RON and MON.

As it is possible to observe in Figure 1, the RON is higher for mixtures rich in branched paraffins and aromatics. The octane number increase with the transformation of linear paraffins into branched paraffins, naphtenes or aromatics and of naphtenes into aromatics.

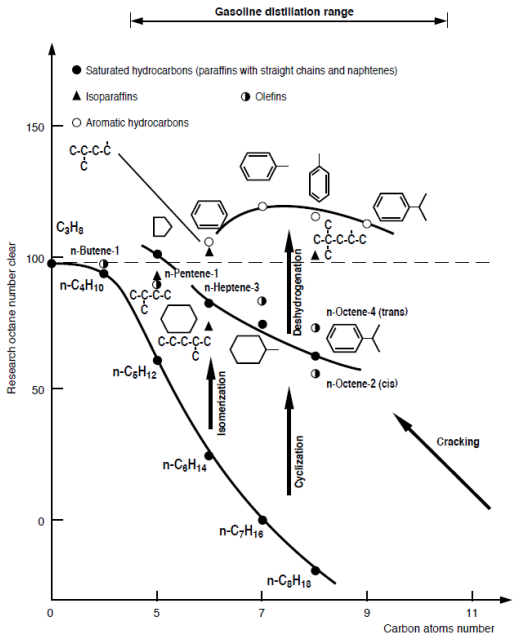

Figure 1 - RON for different carbon atoms number in molecules **[2]**.

2.2 Feed Composition, Characteristics, Products and Reactions

Currently, the FCC process is carried out with a moving bed where the catalyst descends by gravity from a hopper, in the part top of the unit, moves through the reactor and then goes to the regenerator by pneumatic transport. The typical feed is vacuum gasoil (VGO), being possible to have also various types of distillates and vacuum residue.

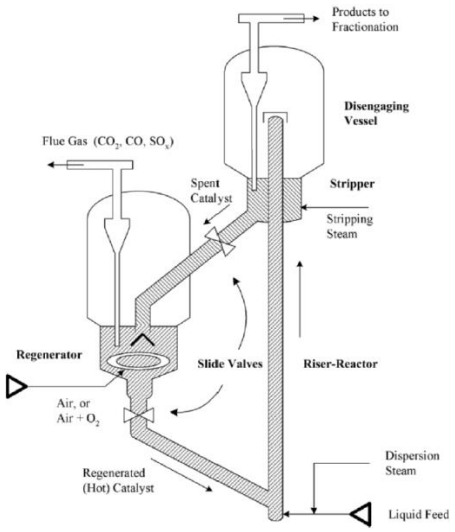

Figure 2 - FCC scheme **[3]**.

The process steps of this unit are divided in three basic functions:

Reaction - Feedstock reacts with catalyst and cracks into different hydrocarbons;

Regeneration - Catalyst is reactivated by burning off coke and recirculated to reactor;

Fractionation - Cracked hydrocarbon stream is separated into various products.

During the reaction step, occurs primary cracking reactions, to promote, such as cracking by β scission (responsible for the formation of olefins) and isomerization (responsible for increasing octane number). Cracking speed depends on the molecule structure and is faster for long chain and for branched paraffins. There are some reactions that should be limited, but not eliminated, such as the hydrogen ion transfer, responsible for the transformation of olefins and naphthenes into aromatics and paraffins stabilizing the gasoline, but at the same time plays an important role in coke formation, and the cycloaddition (Diels – Alder) that forms heavy products and coke.

In the final of the process, cracking products are subjected to a fractionation, resulting in five different streams: Gas (fuel gas/LPG), composed by olefins that can be used in Petro chemistry; Naphtas, boiling range of 160 to 220°C; Light gasoil (LCO), boiling range of 160 to 220-360°C; Heavy gasoil (HCO), fraction that boils between 360 to 550°C; Slurry, the final fraction which boils from 550°C.

The yield of FCC products is higher for gasoline (between 30-60%) followed by Light Cycle Oil (LCO, 10-20%) and Heavy Cycle Oil (HCO, 10-15%).

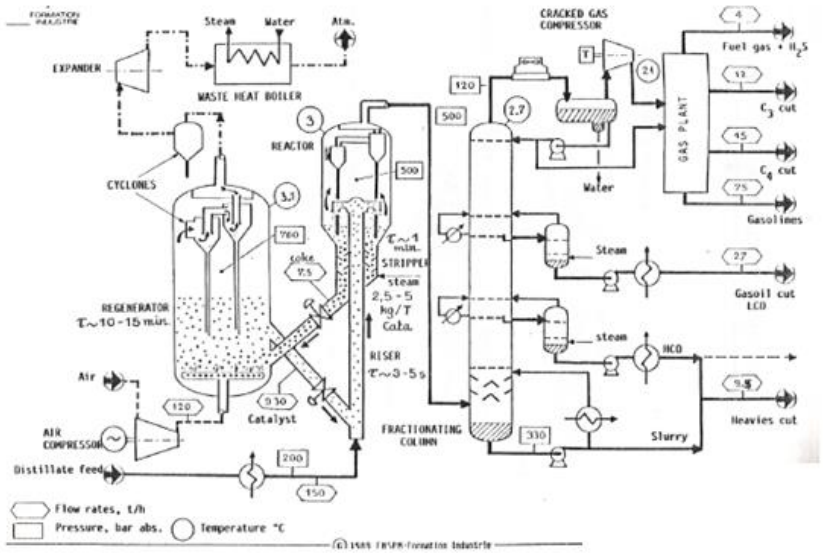

Figure 3 - Overview of FCC unit **[3]**.

2.3 Hydroprocessing Units

In the refineries, there are some feed contaminants which must be removed in hydroprocessing units. This kind of contaminants are related to the crude processed which influences the type of hydrotreatment, and can be present different compounds such as silicon, arsenic, sulphur, metals and aromatics [4]. According to Figure 4, specific treatments are used depending on the compound that is necessary to remove.

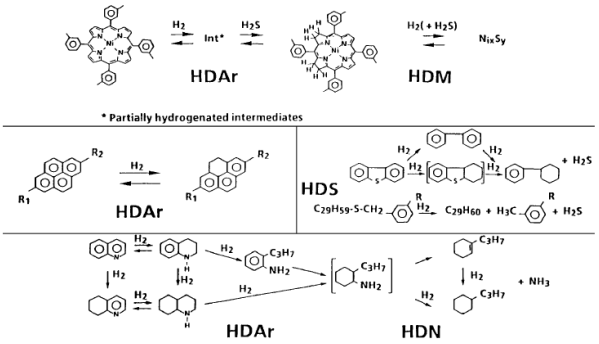

Figure 4 - Different types of hydrotreatment **[5]**.

2.3.1 Desulphurization

Desulphurization units become more and more important in refineries. Catalytic Hydrodesulfurization consists in the transformation of sulfur from molecules to H_2S with high hydrogen pressure, specific catalysts and temperatures between 300 and 400 ^{o}C [6]. The final result are light hydrocarbon compounds formed from sulfur constituents reaction and gas containing H_2S. All the chemical reactions present in this unit have hydrogen consumption, as it is possible to see in the next table.

Table 1 - Hydrodesulphurization reactions **[5]**.

Type	Reaction	ΔH (kcal . mol^{-1})
Mercaptans	$R-SH + H_2 \rightarrow RH + H_2S$	−17
Sulfides	$R-S-R' + 2H_2 \rightarrow R-H + R'-H + H_2S$	−28
Thiophane	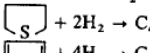 $+ 2H_2 \rightarrow C_4H_{10} + H_2S$	−29
Thiophene	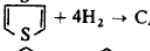 $+ 4H_2 \rightarrow C_4H_{10} + H_2S$	−67
Dibenzothiophene	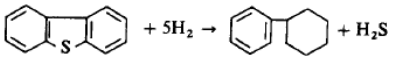	

Hydroprocessing reactions required temperature and hydrogen pressure.

The simplified scheme of a hydrodesulphurization unit is present in Figure 5 and is possible to see the make-up of hydrogen, responsible for the reactions of hydrotreatment, the reactor and the stripper to separate the products.

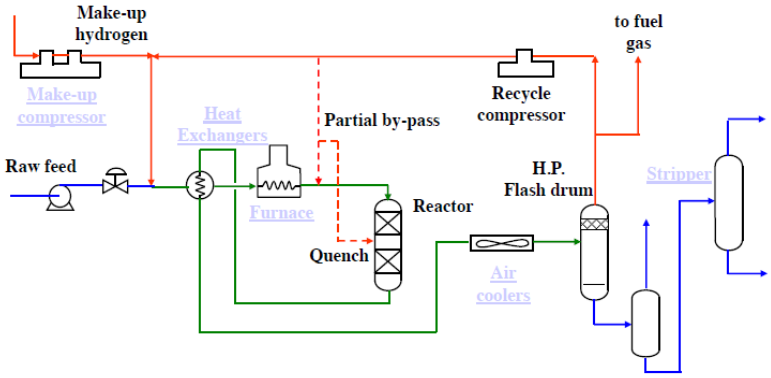

Figure 5 - Scheme of hydrodesulphurization unit **[5]**.

2.3.2 HDS Catalyst

Usually HDS catalysts are constituted by metal oxides from columns VIA (Mo,W) and VIIIA (Co,Ni) of the periodic table. The active phase of this type of catalysts consists in the sulphided form of these oxides – MoS2 slabs. Co or Ni are activity promoters and 'decorate' the edge of MoS2 slabs. If the main objective are HDS reactions with low pressure units, generally CoMo catalysts are used but if the main objective is density and cetane gain (hydrogenation reactions) with high pressure units, NiMo catalysts are used. Oxide catalysts must be sulphided in order to transform the inactive metal oxides into active metal sulphides, with the following type of reactions:

$$MoO_3 + H_2 + 2H_2S \rightarrow MoS_2 + 3H_2O + heat \quad \text{Eq. 1}$$

$$3NiO + H_2 + 2H_2S \rightarrow Ni_3S_2 + 3H_2O + heat \quad \text{Eq. 2}$$

$$9CoO + H_2 + 8H_2S \rightarrow Co_9S_8 + 9H_2O + heat \quad \text{Eq. 3}$$

There are two possibilities to the sulphurization of the HDS catalysts: after loading in the reactor (in situ) and loaded afterwards in the reactor (ex situ).

To do the catalyst activation usually are necessary three different steps: drying, pre sulphurization step and catalyst sulphurization.

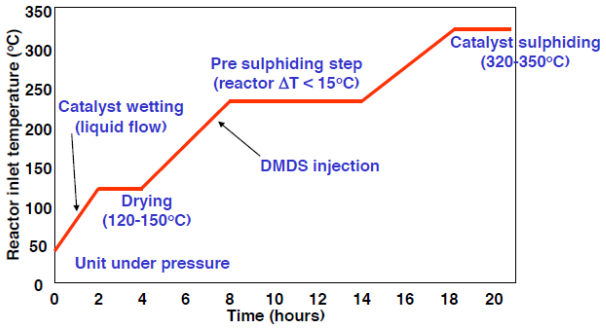

Figure 6 - Catalyst activation **[5]**.

To compensate the catalyst deactivation, the regeneration of used HDS catalysts is possible by carefully burning sulphur and coke. The result is a catalyst in its oxide form.

2.3.3 Dearsenification

Catalytic hydrodesulphurization process of gasoline allows to decrease the sulfur content down to the maximum limit, 10 ppm. Unfortunately, some of these feeds can also contain organo-arsenic compounds, at trace levels, 10-100 ppb, which can be poisons for these catalysts.

2.3.3.1 Dearsenification catalysts

The problematic around the poisoning of the HDT catalysts is recent, thus there is not a lot of available information about this subject.

The catalysts responsible for the dearsenification of feeds are similar to the ones used in hydrotreatment. Alumina-supported nickel catalysts are extensively used in various oleo- and petrochemical processes [7]. These processes include the de-aromatization of commercial solvents and white oils, hydrogenation of pyrolysis gasoline ("pygas"), olefins, edible oils, and aromatic compounds. A new generation of hydrotreating catalysts has been developed which combines a high specific nickel surface area and a high reducibility, indicating a high dispersion and a limited, but effective, metal-support interaction [8]. They are referred to as HTC catalysts.

A highly selective hydrogenation catalyst with limited hydrogenation potential for the conversion of di-olefinic hydrocarbons into mono-olefinic hydrocarbons can be obtained by the partial sulfidation of the nickel [9, 10]. This partial sulfidation step is crucial to remove gum and resin precursors in pygas gasoline, while maintaining a high octane number, for which mono-olefins and benzene derivatives in the gasoline are required. In these partially sulfide catalysts, the surface of the Ni particles is poisoned with a limited amount of sulfur atoms, leading to the desired selectivity.

2.3.3.2 Deactivation of HDT catalysts

According to the literature [11], the activity of HDS catalysts is highly conditioned by the presence of arsenic compounds.

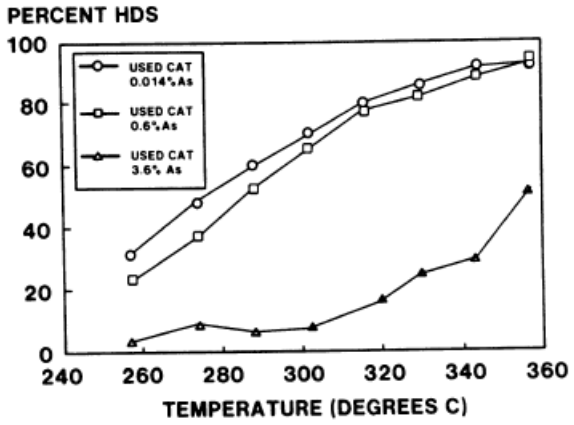

Figure 7 - HDS activity of poisoned plant catalysts **[11]**.

A detailed understanding of the deactivation of CoMo and NiMo hydrotreating catalysts used for desulfurization of hydrocarbon feeds is important to optimize the process parameters in the refineries and to rationalize catalyst research [12]. It's possible to classify this deactivation into four different categories [13]:

1 – Blocking of catalyst pores by coke formation, making the active centers unavailable for reactants;

2 – Sintering of MoS2 slabs;

3 – Poisoning of active sites by strongly absorbing species, which are usually present as N-heterocyclic compounds in the middle and heavier feeds;

4 – Poisoning by deposition of metals, predominantly present in resid feeds, on the active sites.

Poisoning of active sites by nitrogen compounds does not induce structural changes of the active sites and may be reversible by raising the process temperature, instead of the deposition of metals that generally leads to irreversible deactivation. Exposure of CoMo or NiMo hydrotreating catalysts to arsenic containing feedstocks has been recognized to have a dramatic influence on the catalyst activity [14]. Owing to this problem, an arsenic trap material is installed in many hydrotreating reactors in order to prevent any arsenic coming in contact with the hydrotreating catalyst. This "arsenic guard" is usually a supported transition metal (Mo, Co, Ni) oxide/sulfide with a

high tendency to chemisorb largely all the arsenic present in a hydrocarbon stream. Recently, an investigation on an artificially poisoned As-Ni=Al_2O_3 catalyst was published, demonstrating a stepwise poisoning process by the initial formation of surface As adatoms, a migration of these into the Ni particle to form Ni_xAs_y intermetallic phases and the final formation of crystalline NiAs [15, 16]. The formation of Ni_5As_2 and NiAs alloy phases on Ni-reforming catalysts has also been discussed by Nielsen and Villadsen [17]. However, the information currently available in the literature on the chemical state of arsenic after deposition on a NiMo/Al_2O_3 hydrotreating catalyst is very scarce.

The presence of arsenic as arsine and organo-arsenic compounds in petroleum has been recognized to have a significant impact on catalyst activity [14, 15]. The significance of arsenic deactivation can be evidenced by the fact that an arsenic sorbent material is often installed in a guard reactor in order to prevent arsenic contacting the NiMoS hydrotreating catalyst. The arsenic sorbent is typically a supported transition metal sulfide with an efficacy to chemically adsorb arsenic present in the feed stream. Current arsenic removal sorbents are comprised of Ni–Mo supported on Al_2O_3 [18], and effectively remove arsenic from naphtha by sacrificing the nickel to form Ni_xAs_y. However, arsenic can remain in the guard reactor effluent either through incomplete sequestering of the arsenic in the guard reactor or by leaching of arsenic from the sorbent material. The effect can be pronounced with the accumulation of arsenic in the top bed of the naphtha hydrotreater within several months of operation. Arsenic is present in many crude oils in low, ppm or ppb, levels [19]. Compared with the deactivation due to coke and nickel and vanadium metals, deactivation of NiMoS hydrotreating by arsenic is less frequently studied. Several recent studies have reported the deactivation of Ni/Al_2O_3 catalysts using an artificially arsenic concentrated feed stream. These studies have demonstrated that on a Ni/Al_2O_3 catalyst, deactivation proceeds via a stepwise process by the initial population of surface arsenic atoms, the diffusion of these arsenic atoms into the supported nickel particles to form intermetallic Ni_xAs_y phases, and the final formation of crystalline NiAs [15, 16]. Additionally, studies using nickel reforming catalysts have also discussed the formation of Ni_5As_2 and NiAs nickeline alloy phases [17]. However, information regarding the mechanism and chemical state of arsenic after deposition on a NiMoS hydrotreating catalyst is scarce. Considering the significantly lower amount of nickel in the NiMoS hydrotreating catalyst and the unique structure of the bimetallic NiMoS phase, the deactivation mechanism of NiMoS is expected to be considerably different than the mechanism for highly loaded Ni/Al_2O_3 catalysts [20].

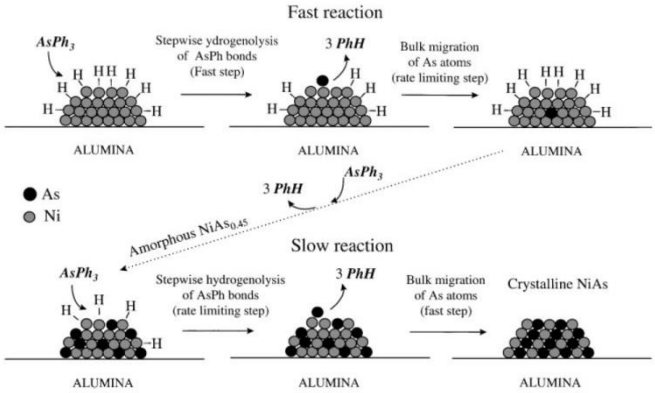

Figure 8 - Catalyst deactivation due to arsenic atoms **[21]**.

2.3.3.3 Reactions of dearsenification with alumina-supported nickel

According to the literature [22], studies about the hydrogenolysis of triphenylarsine with alumina-supported nickel catalysts with various particle sizes were done, under hydrogen pressure and at temperatures ranging from 303 to 443 K.

The reaction initially takes place selectively on the surface of the nickel particles and leads to the successive hydrogenolysis of –As–Ph bonds with benzene and cyclohexane formation. At 303 K, the reaction stops when the Ni particles are completely covered with grafted –As–Ph fragments. The quantity of fixed arsenic increases with the dispersion of the metal particles. It is proposed that more As–Ph fragments (per metallic atom) are grafted onto edge atoms than onto face atoms of the Ni particles. When the reaction is performed at higher temperature, the As atoms migrate inside the nickel particles easily and form an intermetallic compound. At 373 K, the Ni_5As_2 phase, very poorly crystallized, is obtained. At 443 K, the reaction leads to a well-crystallized phase NiAs. The dispersion of the catalyst has no influence on the nature of the formed intermetallic species. However, the formation rate of these species increases with the dispersion of the catalysts. It was demonstrated that triphenylarsine, used as a model compound, reacts readily under hydrogen at 400 K on the metallic surface of alumina-supported nickel, with benzene evolution and formation of As atoms. These As atoms penetrate into the metallic particle to form, in a first step, intermetallic phases Ni_xAs_y and then the well-characterized NiAs nickeline alloy [17]. The interaction between $AsPh_3$ and Ni is typically a reaction of Surface Organo-Metallic Chemistry on Metals [23], which deal with the study and application of reaction between organometallic compounds and metallic surfaces.

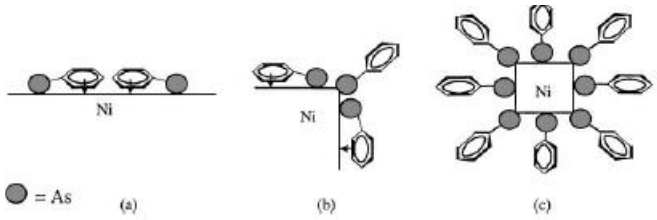

Figure 9 - Models for the adsorption of AsPh3 on Ni/Al2O3: (a) on the faces of the Ni particles, (b) on the edges, and (c) on a very small particle **[22]**.

2.4 Preparation methods of hydrotreatment catalysts

The methods of catalyst preparation have a great influence on the catalytic performance of HDT catalysts, varying the activity, selectivity, stability and mechanical strength.

To perform the preparation, there is two different methods: deposition of the active phase on support already created or addition of the active phase during shaping of support. According to the first way to prepare hydrotreatment catalysts, impregnation and deposition-precipitation can be executed. In the second method, co-precipitation and sol-gel are used. This type of catalysts are very often prepared by dry impregnation and due to that, this topic will be described in more detail.

After the selection of the correct catalyst support and the method of deposition of the active phase, the preparation of HDT catalysts can be divided as:

1) Preparation of metal precursors
2) Deposition of metal precursors on catalyst support
3) Post-treatment
4) Activation

2.4.1 Active phase deposition on support

The goal of this step is to introduce the metal precursor onto porous support. At the same time, a dispersion agent can be added to increase the catalyst dispersion, increasing the activity [24].

2.4.1.1 Dry impregnation of porous solid

The impregnation method consists in the deposition of a solution, with the active metal precursor dissolved in an aqueous or organic solution, in the catalyst support [25]. This technique is used for the synthesis of heterogeneous catalyst, whereby a certain volume of the metal-containing

solution is contacted with the solid support [26]. The added volume is the same as the pore volume of the support. To know which is the volume to add it is necessary to determine the TAPV (total accessible pore volume, cm^3/g) of the support, having two different methods: by mercury porosimetry or doing the same principle than the impregnation but with a solution of potassium permanganate, determining the required volume to fill all the support.

Due to capillary action, the solution migrates into the pores. A step called Maturation is performed in order to ensure a good migration of the salt within all the catalyst pore, inside a recipient filled with water to maintain the humidity constant, avoiding the precipitation of the salt. These first two steps in catalyst preparation influence the amount of the active precursor present on the pores, its concentration profile within the carrier grains and its chemical environment on the support surface [27].

The mass transfer conditions inside the pores during impregnation and drying have an influence on the concentration profile of the impregnated compound. When strong interactions through chemical or physical forces (surface hydrolysis, ligand substitution, ion exchange, electrostatic attraction) between the precursor and the support occur, the amount that remains on the pore walls of the support can be more than the dissolved substance which continues in the pore filling solution. The resulting catalyst is nominated as sorption type [28].

By contrast, without equilibrium conditions, the distribution of the impregnated compound is guided by a sorption-diffusion mechanism and is only slightly affected during drying. The reverse case is that of impregnation-type catalyst. In this case, the dissolved component dominates because of the absence of significant solute-support interaction or because of too large a concentration in the pore solution. The mass transport is responsible for determining the concentration profile during precipitation/crystallization of the dissolved compound that, on the other hand, is controlled by the conditions of the solvent evaporation.

To prepare commercial catalyst with preshaped supports it is essential to control the impregnation profile. Usually, when the sequence of processes at the oxide/solution interface is fast and the diffusion inside the porous structure of the solid is slow, a diffusionally controlled sorption regime happens. If the presence of strong precursor-support interaction is registered, the concentration profiles of the impregnated compounds are, in general, nonuniform. Nevertheless, it is possible to manipulate the way the equilibrium conditions are accomplished by either changing the interfacial chemistry between the impregnant and the support [29] or by using impregnation promoters. Schwarz and Heise proposed a classification system [30] representing the effects of solution ingredients on the ionic strength (changes in the thickness if the electrical double layer at

the interface), on the solution pH (modifying the surface potential and finally partially dissolving the oxide surface) or on the adsorption sites (competing with the precursor species for the same adsorption sites) [27].

2.4.2 Post Treatment and Activation

After impregnation of the metal active phase it is necessary to perform thermal treatments. Calcination and sulphurization are accomplished to transform the active agent into the final form, increasing the dispersion of the active agent. The operating conditions used influence the activity and selectivity of metal supported catalysts. To eliminate the excess solvent present after impregnation, a drying step is done.

2.4.2.1 Drying

This phase consists in the elimination of the excess solvent (usually water) present in the porous solid, subjecting the impregnated catalyst to 90°C in an oven for 3 hours. According to the literature [31], the final characteristics of the catalysts depends on the drying conditions, but also of the chemical environment associated during this step. Drying under vacuum disperses the nitrate precursor on the support, resulting in huge amounts of metal silicates, while prolonged air drying converts the surface silicate into metal oxides.

2.4.2.2 Calcination

Calcination is a heat treatment of catalyst precursor in an oxidizing atmosphere to cause a change in its chemical constitution, without fusion, and influence directly the textural properties of the catalyst such as specific area, porous volume and pore size distribution. Usually, calcination starts with a steady increase in temperature until it reaches a plateau of variable duration. In most part of the cases, an air flow at high temperatures is used, in order to create porosity and to provide mechanical strength to the catalyst [32].

During this step different transformations can happen, such as textural changes by sintering (increasing dimensions of the particles), precursor's decomposition, with creation of active sites and porosity, accompanied by chemical composition changes, modifications in crystal structure and surface cleaning. Large temperature elevations decrease not only the reducibility of the catalysts, but also the metallic dispersion due to the formation of metal silicates and metal aluminates and promotion of sintering effects.

During calcination, the metal nitrate decomposes to a metal oxide [33]. The reaction of oxide formation from nitrate can be explained, for example for nickel, as:

$$Ni(NO_3)_2 \cdot 6H_2O \xrightarrow{450°C} NiO + 2NO_2 + \frac{1}{2}O_2 + 6H_2O \quad \text{Eq. 4}$$

It is important to take in account the temperature of calcination when citric acid is used in the preparation of the solutions, due to the decomposition of this compound. Not being the purpose of this subject to study the decomposition of citric acid according to the metal nitrate used, a typical scheme of calcination for hidrotreatment catalyst was adopted.

2.4.2.3 Sulphurization

Sulphurization is an important stage of the pretreatment of sulfide catalysts for hydrotreatment. This stage is responsible for the control of the active component structure and the catalyst activity.

Oxide catalyst, result form after calcination, must be sulfided in order to transform the inactive metal oxides into active metal sulfides [34]. To perform sulphurization is used a mixture of H_2S/H_2 with a temperature-programmed sulphurization. As temperature rises, the intermediates are reduced in the presence of hydrogen to form MoS2; this process usually starts at the temperature above 300°C. However, at this temperature the sulfiding reaction competes with reduction [35]. For this reason, the catalysts sulfiding needs the formation of intermediate oxysulfide or sulfides at the temperature below 300°C [35, 36].

The sulfiding reaction is exothermic so it is important to control carefully the temperature in order to avoid side reactions that can poison the catalysts, i.e. metallic oxide reduction by hydrogen and coke formation, which would reduce the catalytic activity. For nickel, for example, the reaction is given by:

$$3NiO + H_2 + 2H_2S \rightarrow Ni_3S_2 + 3H_2O + heat \quad \text{Eq. 5}$$

This page was intentionally left blank

3 Experimental Work

Catalysts prepared in this study were supported metal catalysts. In order to test the reactivity of different metals (zinc, copper, nickel, cobalt and iron), solutions with the metal precursors were prepared, applying the preparation method of dry impregnation, the thermal treatment of calcination and the activation by sulphurization. All the prepared catalysts were characterized by different techniques in order to know exactly the textural properties and the catalyst formulation. To study the trapping mass of arsenic, catalytic tests were performed in a batch reactor with the prepared catalysts. Also referenced catalysts were studied, in order to compare the results.

In this chapter are presented the experimental protocols for the catalyst preparation and the description of apparatus used to perform each step, followed by the description of the performed characterization methods as well as their theoretical background and equipment. As a final point, are described the catalytic tests to measure the conversion of the metals.

3.1 Support Characteristics

Two different supports were used to prepare the catalysts: a commercial alumina (AAS: Activated Alumina Support) and a HDS catalyst from *Axens* (composed by cobalt and molybdenum on alumina support). Due to confidential reasons, the specific composition of the *Axens* catalyst can't be detailed. The principal characteristics of the alumina support are presented in Table 2.

Table 2 - Principal characteristics of the commercial alumina support.

Support characteristics	
Shape	Spheres
BET surface (m^2/g)	152
Particle size (mm)	1.5-3
Porous volume (mL/g)	0,71
Average porous size BJH (nm)	18
Volume of water retention (cm^3/g)	1.06
Packing density (g/cm^3)	0.43

3.2 Preparation methods

3.2.1 Preparation and activation methods

Catalysts were prepared by four different methods: dry impregnation, using different metal precursors, followed by drying, calcination and sulphurization. The following figure schematizes the preparation and activation of the supported catalysts.

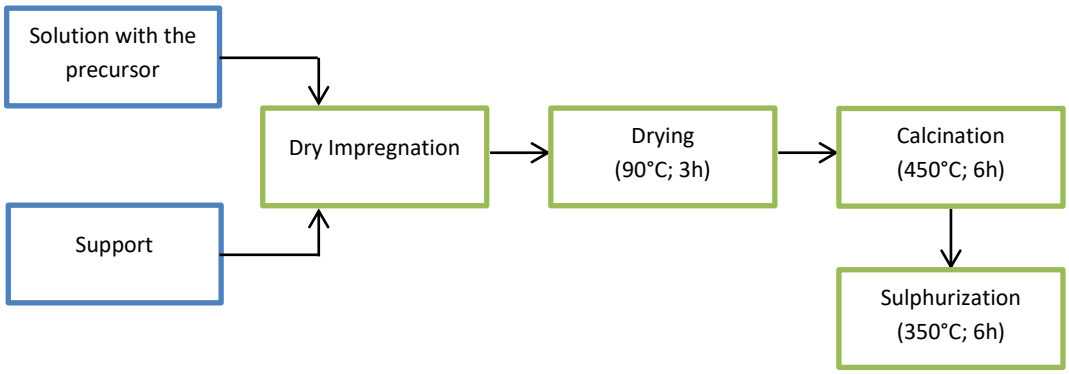

Figure 10 - Scheme of the catalysts preparation and activation.

3.2.1.1 Preparation of the impregnated solutions

The preparation of aqueous or organic solution with an active metal precursor is the beginning for synthesize heterogeneous catalysts. Thus, five different metal nitrates were chosen: zinc nitrate hexahydrate, copper nitrate trihydrate, nickel nitrate hexahydrate, cobalt nitrate hexahydrate and iron nitrate nonahydrate. Thirteen solutions were prepared, the first three by using just water and the metal precursor and the other ones where a dispersion agent was added. To increase the metal dispersion on the catalyst dispersion agents such as citric acid or levulinic acid are used. In this work citric acid is used as dispersion agent.

The addition of citric acid was made in order to obtain a ratio R of 0.8, except for iron for which 0.4 was used, due to solubility problems. The ratio R is equal to:

$$R = \frac{n_{acid}}{n_{metal\ oxide}} \qquad \text{Eq. 6}$$

With,

n_{acid}: Number of mol of acid

$n_{metal\ oxide}$: Number of mol of metal oxide

The number of mol of citric acid is adjusted according to the number of mol of metal oxide.

The impregnation solutions were prepared knowing the metal oxide content desired and the water retention ability of the support, always using 40 g of catalyst support.

To know the amount of metal nitrate, water and citric acid is necessary to:

1) Establish the mass of support to be used
2) Establish the percentage of desired metal oxide:

$$\%metal\ oxide = \frac{mass_{metal\ oxide}}{mass_{support} + mass_{metal\ oxide}} \quad \text{Eq. 7}$$

Thus allowing the determination of the amount of metal necessary.

3) Knowing the quantity of metal, calculate the mass of metal nitrate
4) Determine the quantity of water to add according to the porous volume (TAPV) of the support:

$$Volume_{water} = total\ VRE - Volume_{metal\ nitrate} - Volume_{water\ in\ salt} \quad \text{Eq. 8}$$

5) To add citric acid, the steps are the same except the fourth:

$$Volume_{water} = total\ VRE - Volume_{metal\ nitrate} - Volume_{water\ in\ salt} - Volume_{citric\ acid} \quad \text{Eq. 9}$$

In the following table is presented the summary for the preparations of the solutions to impregnate using the two different supports.

Table 3 - Prepared Solutions.

Type of Support	Catalyst precursor	Percentage of desired metal oxide (%)	
AAS		Without citric acid	With citric acid
	$Zn(NO_3)_2.6H_2O$	-	10
	$Cu(NO_3)_2.3H_2O$	-	10
	$Ni(NO_3)_2.6H_2O$	20	10
	$Co(NO_3)_2.6H_2O$	20	10
	$Fe(NO_3)_3.9H_2O$	20	10
HDS catalyst		With citric acid	
	$Zn(NO_3)_2.6H_2O$	10	
	$Cu(NO_3)_2.3H_2O$	10	
	$Ni(NO_3)_2.6H_2O$	10	
	$Co(NO_3)_2.6H_2O$	10	
	$Fe(NO_3)_3.9H_2O$	10	

In some cases, the concentration of salt for the respective percentage of metal to impregnate exceeds their solubility. In order to ensure that the nitrate is soluble, the amount of the desired metal oxide was reduced. The respective solubility values are indicated in Table 4.

Table 4 - Metal salt solubility in water at 20°C **[37]**.

Salt	Solubility (g salt/100 g water)	Registered solubility (g salt/100 g water)	
$Zn(NO_3)_2.6H_2O$	138*	For 20%	87
		For 10%	39
$Cu(NO_3)_2.3H_2O$	125	For 20%	72
		For 10%	32
$Ni(NO_3)_2.6H_2O$	94	For 20%	92
		For 10%	41
$Co(NO_3)_2.6H_2O$	97	For 20%	92
		For 10%	50
$Fe(NO_3)_3.9H_2O$	138	For 20%	119
		For 10%	53

*value for 30°C

3.2.1.2 Experimental conditions and apparatus

Dry impregnation was performed in the equipment shown in Figure 11. It consisted of a metal support where the glass recipient is placed with the catalyst support, which was rotating due to a stirring motor at a velocity of 60 rpm. The precursor solution present in a buret was introduced dropwise, mixing the catalyst and the solution with the aid of a metal spatula.

Figure 11 - Dry impregnation.

In order to obtain a homogeneous distribution of the precursor solution over the support, the impregnation step was performed in around 40 minutes for the alumina support and 25 minutes for the HDS catalyst from *Axens*.

After impregnation, the catalyst was subjected to drying in order to eliminate the excess solvent (usually water) present in the pores of the solid, putting the impregnated catalyst in the oven for 3 hours at 90°C.

To perform calcination, it is important to take in account the mass of support used for the impregnation, the WHSV (weight hourly space velocity) and the PD (packing density).

To determine the packing density of the support is required a graduated cylinder, measuring the volume of the support and the correspondent mass. Therefore, the volumetric air flow to use is given by:

$$Volume_{solid} = \frac{mass_{support}}{PD} \quad \text{Eq. 10}$$

$$flow_{air} = WHSV \times Volume_{solid} \quad \text{Eq. 11}$$

Calcination was performed with an WHSV of 1500 h^{-1}, under an air flow of 139 NL/h for the catalysts supported by alumina and with 112 NL/h for the catalysts from *Axens*, in a tubular four equipped with a glass reactor which had a porous plant, controlled by an electronic system where is introduced the air flow and the temperature evolution, according to the Figure 12.

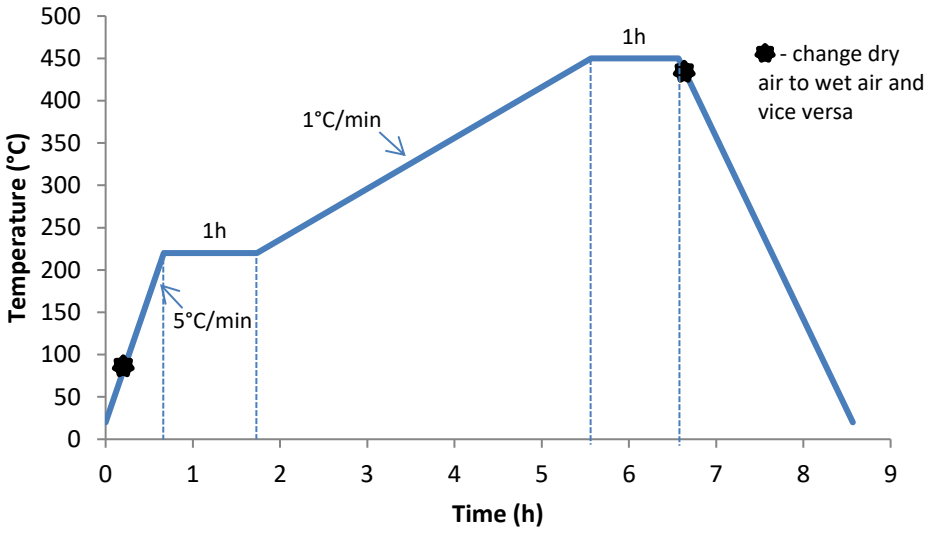

Figure 12 - Calcination profile used for all catalysts.

This program of calcination was applied to all catalysts.

In order to activate the metal phase of the catalyst, sulphurization was performed using 3g of each catalyst. A pressure of 2 bar was used in this step.

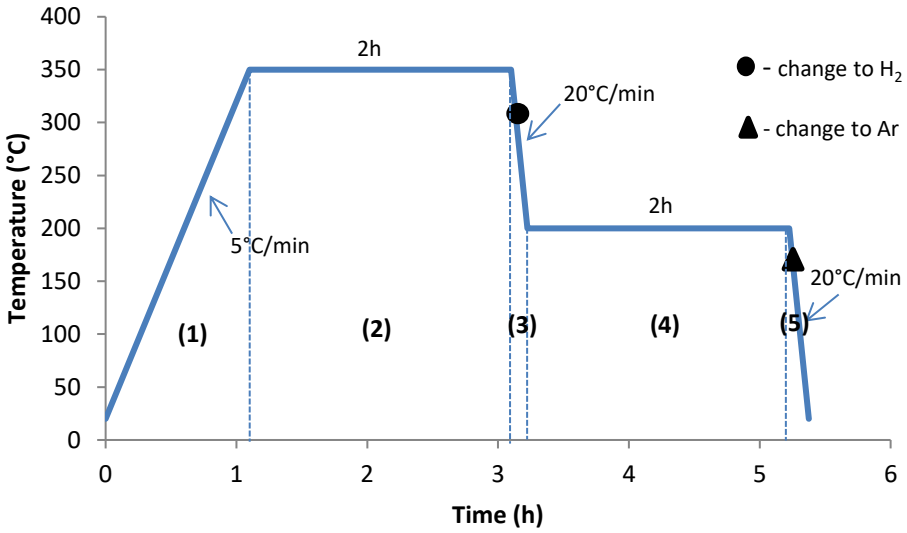

Figure 13 - Sulphurization profile used for all catalysts.

As can be seen in Figure 13, the sulphurization process is composed by 5 steps:

- It begins with a temperature ramp from the room temperature to 350°C, under H_2S/H_2 (15%H_2S) flow of 1 nL/h/g_{cat} **(1)**;
- Then this temperature is maintained in order to produce the sulfide form of the catalyst **(2)**;
- After that there is a temperature decreasing to 200°C, under H_2 flow of 1 nL/h/g_{cat} **(3)**;
- The temperature is maintained in order to reduce the catalyst and remove the reactive sulfur species (S^{2-},SH^-,S_2^{2-}) [38] **(4)**;
- To finish, the temperature is decreased until the room temperature, under Ar flow **(5)**;

In order to ensure that the sulphurization was completely performed, the number of mol of H_2S used and the number of mol of metal in the different catalysts were compared. The results are present in Table 5.

Table 5 - Comparison between the metal and the metal sulfide mol.

Type of catalyst	Metal mol (mmol/3 g_{cat})	H_2S mol (mmol/3 g_{cat})
Metals on alumina	7	63
Metals + citric acid on alumina	3	
HDS catalyst	7	
RC2	7	
RC1	12	

As can be observed in the previous table there is an excess of H_2S comparatively with the amount of metal present in the catalysts, meaning a complete sulphurization of all of them.

In the final of step 5, vacuum is applied in order to allow the cut of the cell, resulting in a closed glass cell with the sulphided catalyst.

This classical profile of sulphurization for HDS catalysts was adopted, not being the purpose of this subject the study of different profiles or conditions of sulphurization.

Thus, were used always the same activating conditions in order to be sure that the catalysts performances were only depending on the test conditions and not the activation procedure.

3.3 Characterization methods

Different analysis were performed in order to describe the structure of the catalysts and their precursors, allowing the identification of the active sites activate and revealing possible ways to improve the catalyst structure [39]. The characterization methods used were: N_2 adsorption-desorption, mercury porosimetry, X-ray diffraction (XRD) and X-ray fluorescence (XRF).

3.3.1 N_2 adsorption-desorption

Nitrogen adsorption-desorption is a characterization technique used to study the textural properties of catalyst supports in the micro (less than 2 nm) and mesopore range (between 2 and 50 nm), following the adsorption phenomenon [40].

Adsorption equilibrium is characterized by isothermal plots which describe the amount of adsorbed gas on the solid surface at a given temperature as a function of the equilibrium pressure of the gas in contact with the solid [41].

Before the determination of the adsorbed quantities, a pre-treatment is carried out in order to remove the compounds adsorbed on the surface of the sample, such as water or carbon dioxide. To accomplish that, the sample is subjected to vacuum and then the temperature is increased. Subsequently, the sample is placed in a tube submerged in liquid nitrogen at 77 K, a feeble nitrogen pressure is produced and the adsorbed volume is measured. Due to the gradually increasing of pressure, it is possible to obtain the adsorption isotherm.

The smallest pores are filled first followed by the condensation of gas in consecutively larger pores until the saturation level for the corresponding vapor pressure is reached at which the entire porous volume is saturated with liquid. To obtain the desorption isotherm, are taken measures of the quantities of gas which remains adsorbed by decreasing relative pressure levels. The analysis were performed on a *Micrometrics ASAP 2420* equipment.

According to IUPAC the shapes of the isotherms and hysteresis loops can be classified, relating the form of the isotherms, the average radius of the pores and the intensity of the adsorbate-adsorbent interactions.

The analysis of these isotherms can be made by using the BET model, *t*-plot or the BJH method, for example. BET model is used to determine the specific surface area of solids, while *t*-plot is a simple method which consists on the comparison between the adsorption isotherms of a given solid related to the adsorbed layer thickness. BJH method plots the curve of derivative of the adsorbed volume as a function of pore diameter in order to obtain the porous distribution.

For this specific work, the most important characteristics are the specific surface area of the catalysts and the total porous volume, using the BET model based on the following equations:

$$\frac{\mathrm{P}}{\mathrm{V}(\mathrm{P}_0-\mathrm{P})} = \frac{1}{\mathrm{V_m C}} + \frac{\mathrm{C}-1}{\mathrm{V_m C}}\frac{\mathrm{P}}{\mathrm{P}_0} \qquad \text{Eq. 12}$$

With,

P: Equilibrium pressure

P_0: Saturation pressure

V: Adsorbed gas quantity

V_m: Monolayer adsorbed gas quantity

C: BET constant

$$S_{BET} = \frac{NAV_m 10^{-20}}{mV_M}$$ Eq. 13

With,

S_{BET}: Specific surface area

N: Avogadro's number

A: Area occupied by an adsorbed molecule

V_m: Monolayer adsorbed gas quantity

V_M: Molar volume at standard conditions

m: Mass of the sample

The results obtained by this method are presented in the next table.

Table 6 – Nitrogen adsorption-desorption results.

Catalysts	S_{BET} (m^2/g)	Total porous volume (cm^3/g)
Nickel on alumina	108±5.4	0.516±0.010
Cobalt on alumina	115±5.8	0.556±0.011
Iron on alumina	136±6.8	0.527±0.011
Zinc on alumina⁺	124±6.2	0.625±0.013
Copper on alumina⁺	124±6.2	0.620±0.012
Nickel on alumina⁺	134±6.7	0.556±0.012
Iron on alumina⁺	136±6.8	0.582±0.012

+ prepared with an aqueous solution with citric acid

The use of the dispersion agent increases 24% the specific surface area for nickel catalysts in relation to the catalyst prepared without citric acid. The total porous volume increases too for this catalyst but also for the iron catalyst: an increase of 8% for nickel and 10% for iron.

The average specific surface area of alumina impregnated only with a solution of metal precursor is 120 m^2/g and for alumina impregnated with the solution with citric acid is 131 m^2/g. The total porous volume is 0.533 cm^3/g and 0.597 cm^3/g, respectively. These average values are typical values for the commercial alumina AAS.

3.3.2 Mercury porosimetry

Mercury porosimetry also allows the textural characterization of catalysts with the determination of the specific surface area and pore size distribution. As opposed to nitrogen adsorption-desorption, this technique is generally applied for macroporous samples and for the upper range of mesoporous (3,5-50 nm) [41].

To perform Hg porosimetry, an external force, applied pressure, is used to accomplish the penetration of a non-wetting liquid, in this case mercury, in the pores. This force counters the resistance created by the surface tension of the liquid. The Washburn's equation gives the pore size corresponding to the applied intrusion pressure:

$$r_p = \frac{-2\gamma cos\theta}{P} \qquad \text{Eq. 14}$$

With,

r_p: Pore radius corresponding with the applied pressure

P: Applied intrusion pressure

γ: Surface tension of the absorptive

θ: Contact angle with the pore surface

The principle behind this technique consists in the measure of the decrease in the quantity of liquid due to penetration into the pores as a function of the applied pressure, is possible to have a distribution of the porous volume versus the pore size. Initially, the sample is prepared by degassing in an oven under standardized conditions and is subjected to a low pressure treatment, followed by a high pressure phase (4000 bar). According to the porosity of the solid under examination, the pressure is increased in stages. With the increasing of the pressure, the smaller pores become filled. To perform mercury porosimetry was used a *Micrometrics Autopore IV 9500*.

Different graphs are obtained by this technique, corresponding to the cumulate volume of mercury penetrated as a function of pore diameter logarithm and to the derivate of this curve as a function of pore diameter.

The porous volume and the average pore diameter are similar for all catalysts.

The contribution of accessible macropores to the total pore volume is negligible in comparison to the pore volume of mesopores.

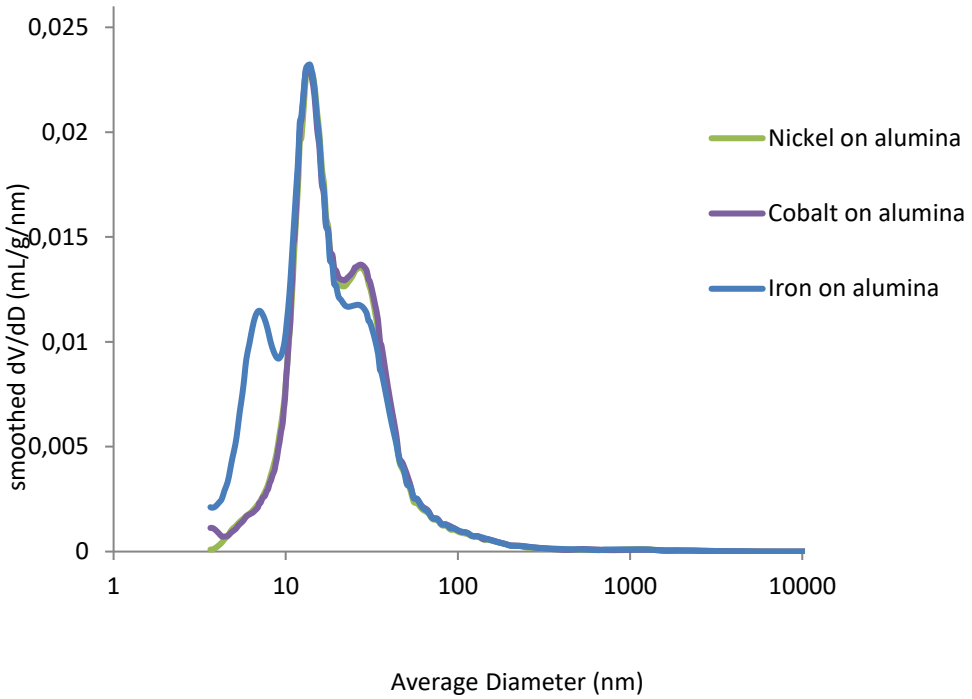

Figure 14 - Mercury intrusion for the catalysts prepared with an aqueous solution.

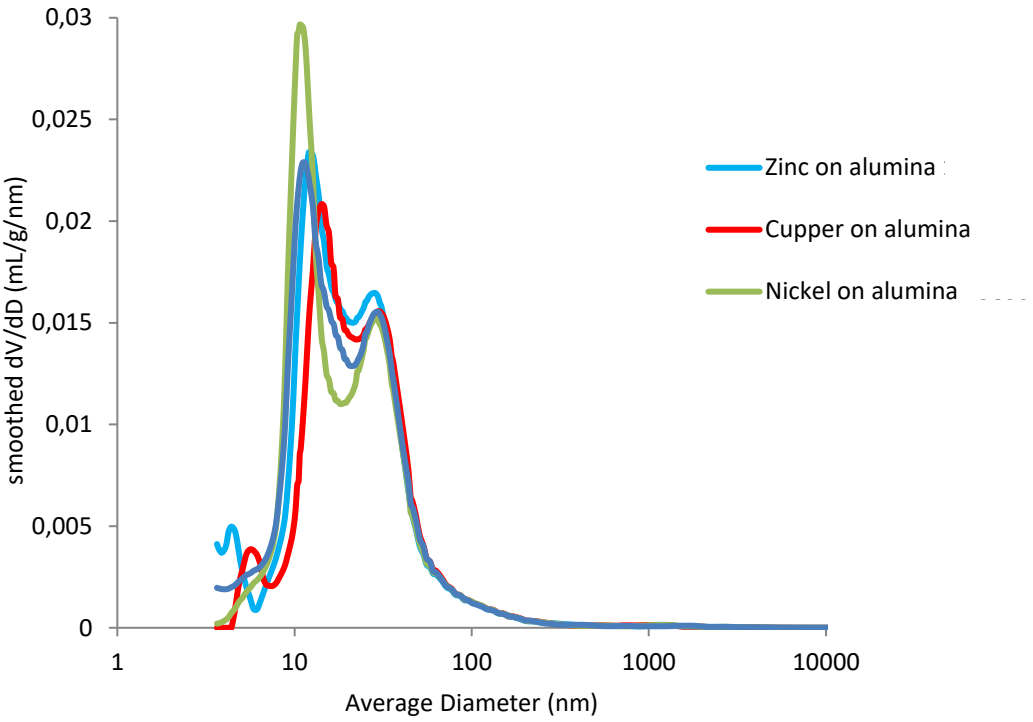

Figure 15 - Mercury intrusion for the catalysts prepared with an aqueous solution with citric acid.

The pore diameters and pore volumes are present in Table 7.

Table 7 - Important results from mercury porosimetry.

Catalysts	Pore Volume for diameter < 7 µm (cm^3/g)	Pore diameter at max dV/dD (nm)	Macropore volume (cm^3/g)	Mesopore volume (cm^3/g)
Nickel on alumina	0.85±0.02	13.8	0.35±0.04	0.48±0.02
Cobalt on alumina	0.86±0.02	12.8	0.35±0.04	0.48±0.02
Iron on alumina	0.86±0.02	13.4	0.36±0.04	0.49±0.02
Zinc on alumina⁺	1.02±0.02	11.6	0.42±0.04	0.57±0.03
Copper on alumina⁺	0.98±0.02	13.7	0.42±0.04	0.54±0.03
Nickel on alumina⁺	1.00±0.02	10.6	0.43±0.04	0.54±0.03
Iron on alumina⁺	1.02±0.02	10.8	0.43±0.04	0.55±0.03

+ prepared with an aqueous solution with citric acid

Comparing the influence of the dispersion agent, the pore volume of the catalysts (for a diameter less than 7 µm) increases 18%, the pore diameter at maximum dV/dD decreases around 21%, the macropore volume increases 20% and the mesopore volume increases 13%, in relation to the catalysts prepared without citric acid. The pore diameter at maximum dV/dD decreases around 21%.

The average pore volume (for a diameter less than 7 µm) of alumina impregnated only with a solution of metal precursor is 0.86 cm^3/g and for alumina impregnated with the solution with citric acid is 1.01 cm^3/g. The pore diameter at maximum dv/dD is 13.3 nm and 11.7 nm, the macropore volume is 0.35 cm^3/g and 0.43 cm^3/g and the mesopore volume is 0.48 cm^3/g and 0.55 cm^3/g, respectively.

3.3.3 X-Ray Diffraction

X-Ray diffraction is a technique used to analyze the elemental properties of a crystal, which normally allows the identification of crystallite phases and the evaluation of the crystallite sizes, according to their degree of crystallization. The principle behind this technique is given by Debye-Scherrer equation [39], which relates the angular bready β of a diffraction line:

$$\beta = \frac{C\lambda}{Lcos\theta} \qquad \text{Eq. 15}$$

With,

C: Bragg constant

λ: X-Ray wavelength

L: Volume-average size of crystallites

θ: Bragg angle

The “integral width” or the full-width half-maximum (FWHM) can be used for determine the peak breadth. In this case, the FWHM was used.

The way that the peak breadth is measured influence the value of the Bragg constant, C. Furthermore, the crystallite sizes are measured for a plane characterized by the Miller indices hkl.

X-Ray diffraction is not very sensitive to the presence of very small particles (<2-3 nm), only if the peaks are getting too broad to be identified and measured. The presence of strained and imperfect crystals and the finite size of crystallite have impact on the broadening XRD lines [39].

This technique is based on constructive interference of monochromatic X-rays and the catalyst sample. The diffraction phenomena is only observed for a certain number of crystallites which present a given group of planes (hkl) to the beam with an incidence angle compatible with the Bragg condition. The results are obtained by the angular positions as a function of the intensities of the resultant diffracted peaks [41].

The results obtained for the studied samples were measured on a *PANalytical X'Pert PRO* diffractometer instrument, in a reflection configuration (Bragg-Brentano) with a stationary X-Ray source and a movable reactor. To perform that, the samples (0.5 g) were prepared by powder compaction.

The diagrams were scanned at 0.05°/step, using 5 seconds acquisition time per step and the analysis range was from 5 to 72° (2θ). The software used to obtain the diffractograms was *DiffracPlus* commercialized by Siemens/Socabim. For nickel oxide on alumina, the results demonstrate the presence of NiO with a measured angle for determine the crystal size of 43.3° (2θ). The crystal size obtained was 154±15 Å.

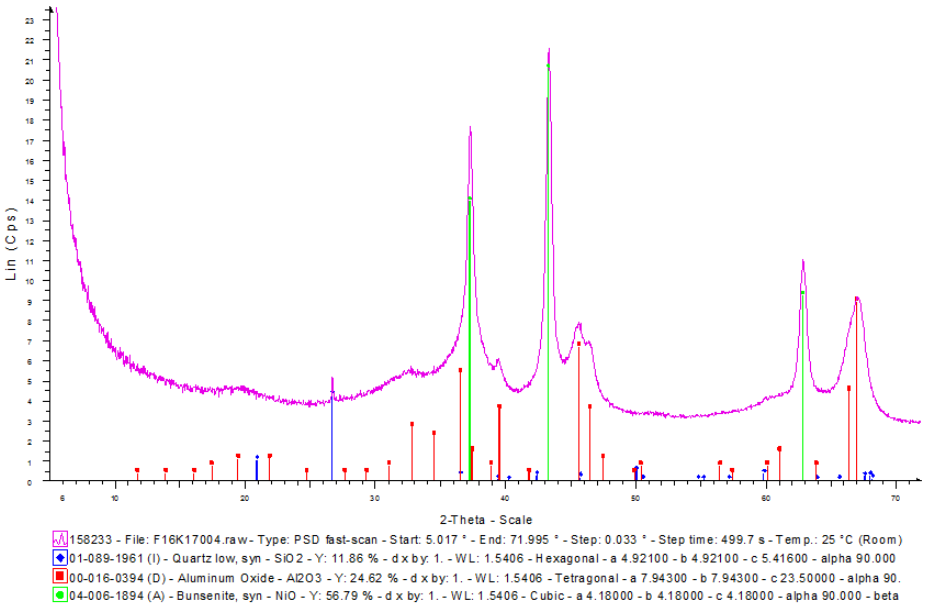

Figure 16 - XRD results for nickel oxide on alumina.

The remaining results for all prepared catalysts are present in **Appendix I**.

3.3.4 X-Ray Fluorescence

In order to determine the elemental mass loadings, X-Ray Fluorescence was used. This technique is based on excitation using an X-Ray tube. The X-Ray emitted from the excited atoms relaxation provides information on the composition of the sample. This type of information is related to the energy of the characteristic rays, that allows to identify the nature of the sample-containing elements, and it's measured the intensity which depends on the mass concentration level of the element for a given energy level [41].

The elemental mass loadings obtained for the studied samples are present in Table 8, measured on a Thermo Scientific instrument, model Advant'X ARL.

Table 8 - Metal content obtained by X-Ray Fluorescence.

Catalysts	Metal (wt. %)
Nickel on alumina	14.56±0.47
Cobalt on alumina	13.79±0.45
Iron on alumina	10.82±0.26
Zinc on alumina[+]	7.49±0.39
Copper on alumina[+]	7.48±0.39
Nickel on alumina[+]	7.34±0.26
Iron on alumina[+]	6.29±0.19

+ prepared with an aqueous solution with citric acid

3.4 Catalytic tests

Catalytic tests for dearsenification of organo-arsenic compounds were carried out in a batch reactor. The metal catalysts previously prepared and some catalysts from *Axens* (RC1 and RC2) were tested. RC1 is composed by nickel, cobalt and molybdenum and RC2 by nickel, all of them on alumina support. A simple model feed was used in order to study the conversion of organo-arsenic compounds. Details of the preparation of the feeds, experimental tests and protocols are presents in the following sections.

3.4.1 Preparation of the concentrated feeds

To perform the tests in the reactor, different solutions of organo-arsenic compounds were prepared. It is possible to divide them in two different groups according to the chemical compound involved: triphenylarsine and triethylarsine. To prepare this solutions, toluene was used as solvent.

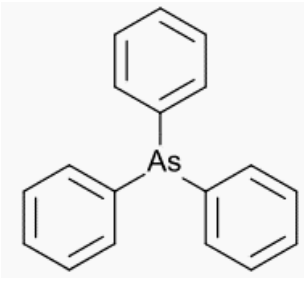

Form: solid

Molecular Weight: 306.23 g/mol

Density: 1.395 g/cm^3

Melting Point: 58-61°C

Boiling Point: 373°C

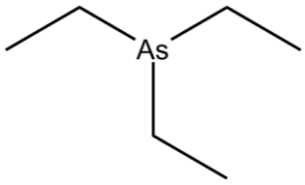

Form: liquid

Molecular Weight: 162.10 g/mol

Density: 1.152 g/cm^3

Melting Point: -91°C

Boiling Point: 140°C

Figure 17 - Properties of Triphenylarsine and Triethylarsine **[42, 43]**.

In Table 9 is presented a summary of the prepared solutions with different arsenic concentrations according to the metal content present in the catalyst.

Table 9 - Concentrated feeds prepared solutions.

Type of catalyst	Concentration (ppm As)	
	$AsPh_3$	$AsEt_3$
Metal	-	6500
Metal + citric acid	2155*	3000
HDS + Metal + citric acid	215.5	2155*
RC1	2155	2155
	215.5	215.5
RC2	2155	2155
	215.5	215.5

* only for Nickel

3.4.2 Description of the experimental unit (T230)

The tests were performed in the Grignard reactor T230 (Figure 18), closed, stirred and under hydrogen pressure. The main objective of this unit is to determine the activity and selectivity of catalysts, according to representative molecular models of a FCC gasoline.

Figure 18 - Grignard reactor T230.

This type of reactor allows to operate with small quantities of feeds and catalysts. The tests are performed during one day permitting a rapid screening of catalysts. The Figure 19 shows a very simplified scheme of T230 unit.

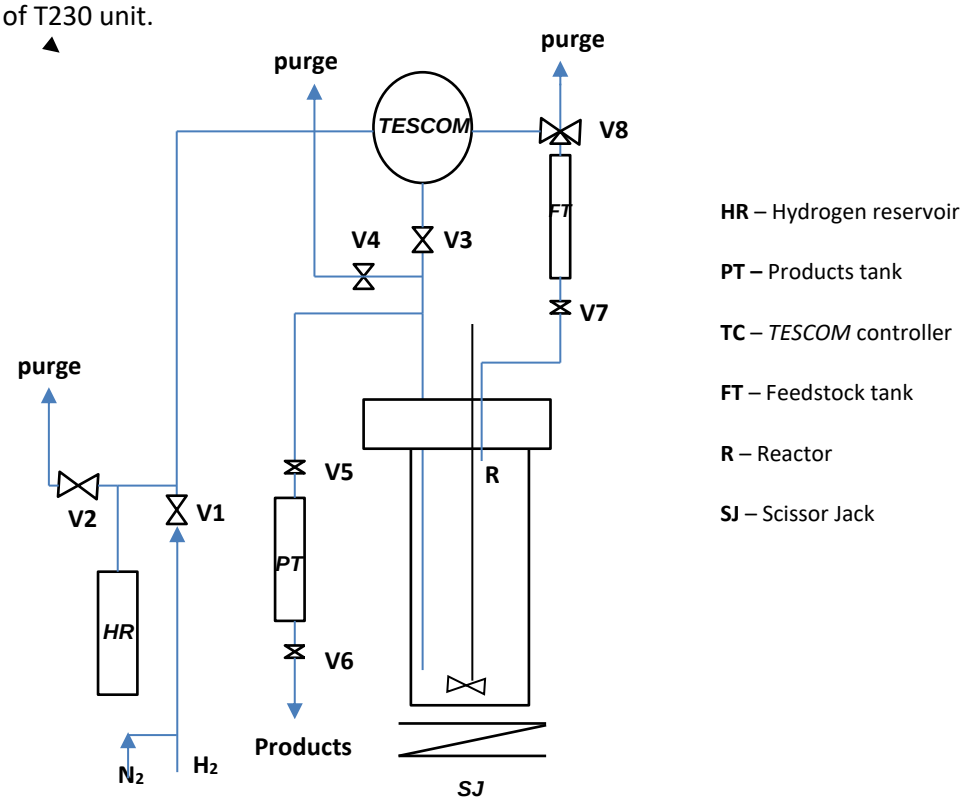

Figure 19 - Simplified scheme of T230 unit.

The Grignard reactor has a total volume of 500 mL and the stirring was performed at a rate of 1000 rpm. The reactor is covered by a heated shell which is controlled and regulated by a set of thermocouples: a measuring thermocouple that also works as a control thermocouple, and a security thermocouple.

The temperature regulation of the reactor is accomplished by a PID controller (*EUROTHERM 2416*). The power control is done by a *thermocouple TKA 10×25*.

The test pressure is controlled by using a *BROOKS* pressure type regulator or a *TESCOM* pressure regulator (present in Figure 19).

The liquid feed is stocked in the tank (FT) of 50 mL, pressurized by a line of hydrogen regulated by the *TESCOM* pressure regulator. The transport of the liquid from the tank to the reactor inlet is done by gravity.

The heating necessary to obtain an isothermal profile through the reactor is provided by an oven.

At the outlet there are two valves which allow the taking of the liquid samples of the reaction.

3.4.3 Start-up and loading of the reactor

The loading of the reactor was done by the introduction of the catalyst and the solvent, performed in a glove box to avoid contact with air (possibility of oxidation).

The mass of catalyst introduced in the reactor was 3 g and 220 mL of solvent are used. To introduce the catalyst inside the reactor is used a basket, schematized in Figure 20.

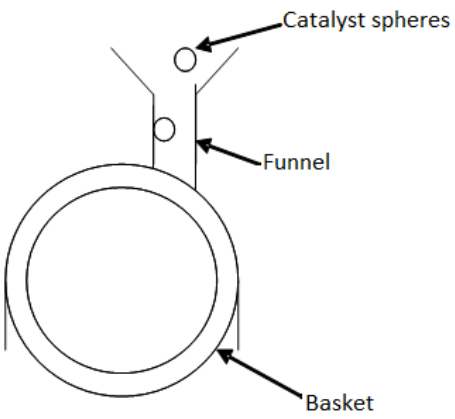

Figure 20 - Scheme of catalyst filling in the basket.

Then, a purge of the unit is done in order to release all the air (O_2) present in the lines of the unit, avoiding the reaction of oxygen with the activated catalyst. At the end of the purge and after the pressure stabilization in the reactor and in the hydrogen reservoir at 35 bar and 50 bar, respectively, a pressure test under nitrogen flow is performed during 2 hours to check the leaks, with a decrease tolerance of 0.1 bar maximum per hour. After that, the pressure was decreased to 2 bar and the reactor was started to be stirred and heated until 250°C, setting the pressure of the reactor at 35 bar and the pressure of the hydrogen reservoir at 50 bar, after complete heating. During the heating and stirring, 30 mL of the concentrated feed were introduced in the feedstock tank.

When is reached the test temperature (250°C) the valve V7 is opened for the entrance of the feed in the reactor, starting the reaction.

Thus, the preparation of the reactor usually takes 4 hours and comprises the following steps: loading of the reactor, purge of the unit, pressure test and heating and stirring.

3.4.4 Liquid product analysis

The reactor liquid effluents were analyzed by gas chromatography, with data acquisition performed by the software *Galaxie*, in order to follow the concentration evolution of the arsenic compounds in the solvent, determining the conversion of the reaction. To perform this, few samples were taken with different reaction times (in minutes): at t=0 (when is introduced the concentrated feed inside the reactor); t=5; t=10; t=15; t=20; t=30; t=40; t=50; t=60; t=75; t=90; t=120. A sample of the concentrated feed was also taken in order to know the initial concentration of the arsenic compound and compare with the different concentrations over the time.

The arsenic conversion corresponds to the arsenic quantity trapped in the catalyst. The quantity of organo-arsenic compound is proportional to the peaks areas obtained by gas chromatography. The arsenic conversion was obtained from the ratio between the quantity of arsenic present at the taken samples and the initial quantity of arsenic in the concentrated feed.

3.4.5 Catalyst and final purified liquid analysis

After the reaction, 100 mL of the final liquid remained in the reactor and the catalyst were submitted to analysis. The liquid was submitted to X-Ray Fluorescence, in order to know the total arsenic content, to ensure that this total arsenic amount is in agreement with the gas chromatography results (meaning that it does not occur the formation of secondary arsenic species such as diphenylarsine and all the content correspond to arsenic trapping) and to Gas

Chromatography and Mass Spectrometry to identify the arsenic species formed after reaction. The catalyst was submitted to X-Ray Fluorescence to discover the arsenic content in the solid.

However, the liquid analysis are delayed and cannot be presented in this report.

This page was intentionally left blank

4 Results and Discussion

4.1 Characterization of the solids after calcination

4.1.1 Zn, Cu, Ni and Fe catalyst

The results for the catalysts constituted by zinc, copper, nickel and iron were previously explained in **chapter 3.3**.

4.1.2 Case of cobalt catalyst

Following the calcination profile explained in the **chapter 3.2.1.2** was observed the formation of two different colors in the spheres of the cobalt precursor catalysts prepared with citric acid, as it is possible to see in Figure 21.

Figure 21 - Formation of two different color spheres after calcination.

In the final of calcination, inside the quartz cell of calcination, the catalyst bed was black in the top, bottom and in the walls, being blue inside of the bed.

In order to identify the reason of this case, the following steps were performed:

1) Selection of two spheres, one black and one blue, and smash them to check the inside color.

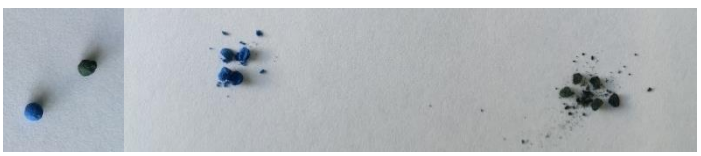

Figure 22 - Blue and black spheres before and after smash.

Analyzing the Figure 22, it is possible to conclude that the color inside the spheres is the

same than in the external surface. According to this fact, the possibility of coke formation is negligible.

2) Loss of ignition analysis for two samples, one with black spheres and the other one with blue spheres, were performed following the loss of weight with the increasing of temperature, in order to know if the calcination was incomplete.

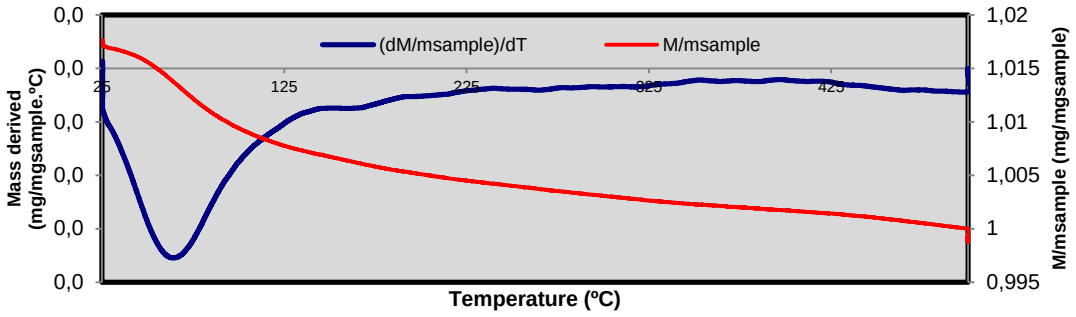

Figure 23 - Mass derived profile in function of temperature for blue spheres.

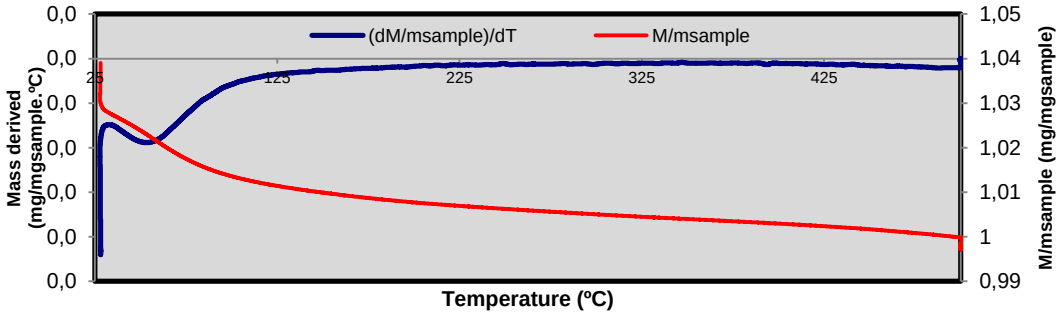

Figure 24 - Mass derived profile in function of temperature for black spheres.

The results demonstrate that for blue and black spheres the loss of weight is 0.03 mg/mg sample and 0.06 mg/mg sample, respectively. This proves that the calcination was not incomplete and, due to the negligible amount of weight lost, there may be the formation of new species beyond the cobalt oxide.

3) XRD analysis were performed to discover which species are present in the final sample of calcination (mixture of blue and black spheres).

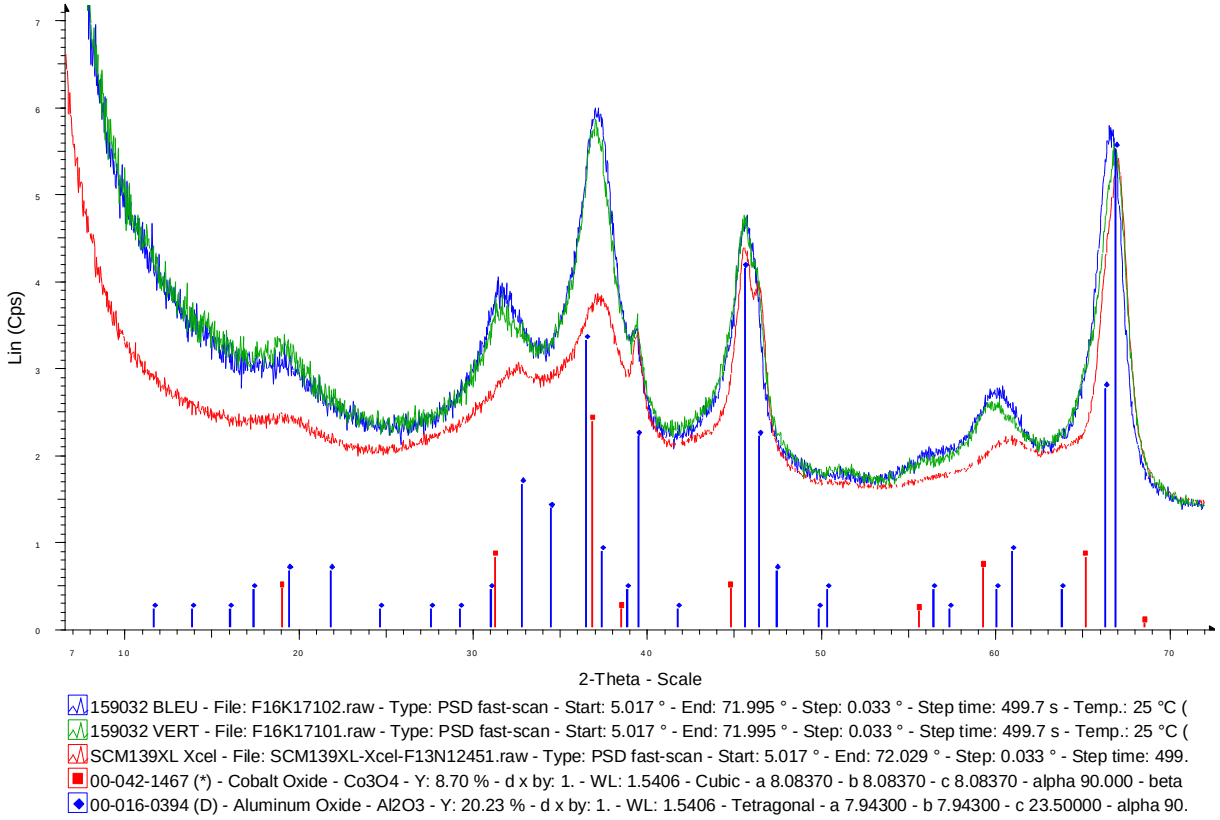

Figure 25 - XRD results.

The results show the integration of cobalt into the structure of the alumina and the formation of cobalt aluminate, explaining the blue color of the spheres.

4) To avoid the formation of cobalt aluminate during the calcination, XRD "*in-situ*" was performed in order to determine at which temperature occurs the formation of this aluminate.

   From the environmental temperature to 150˚C, it is detected the presence of cubic gamma alumina as can be seen in Figure 26 and Figure 27.

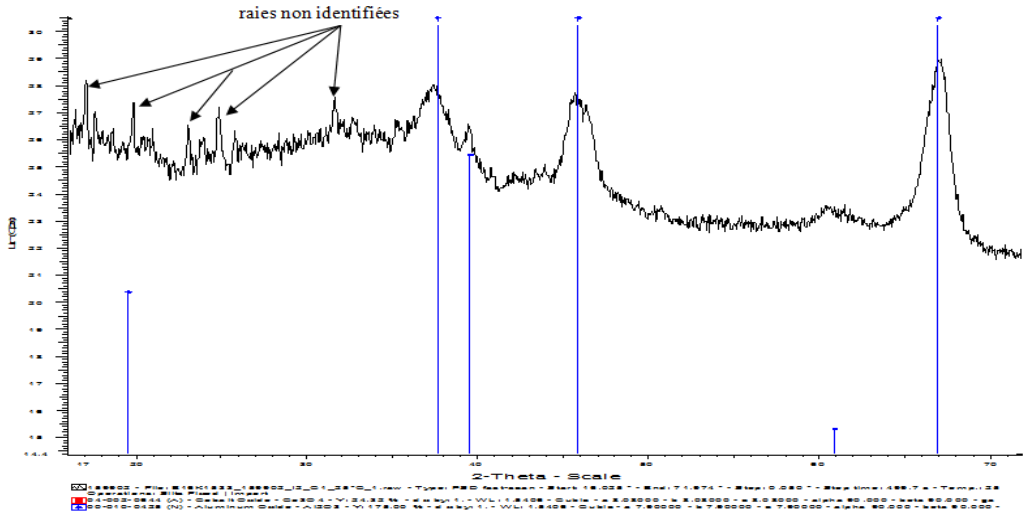

Figure 26 – XRD *'in-situ'* results for 25˚C.

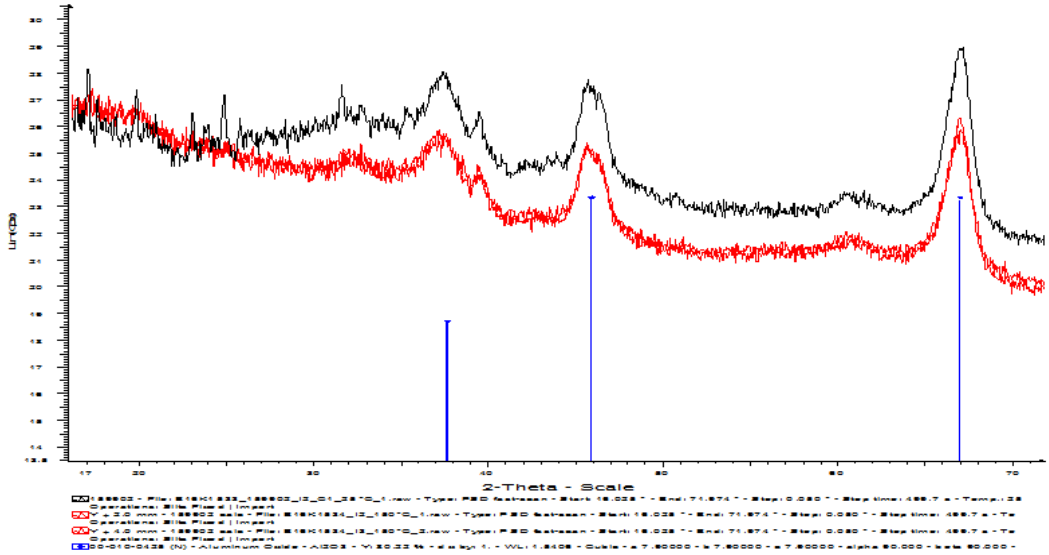

Figure 27 - XRD *'in-situ'* results for 25˚C (black) and 150˚C (red).

From 200˚C to 350˚C is detected the presence of Co_3O_4, increasing the signal with the increasing of temperature. The signal of Co_3O_4 is so large that it means the formation of small crystals of this compound. At 350˚C is identified a supplementary ray towards 26.5˚2θ which corresponds to carbon, from the decomposition of citric acid (Figure 28).

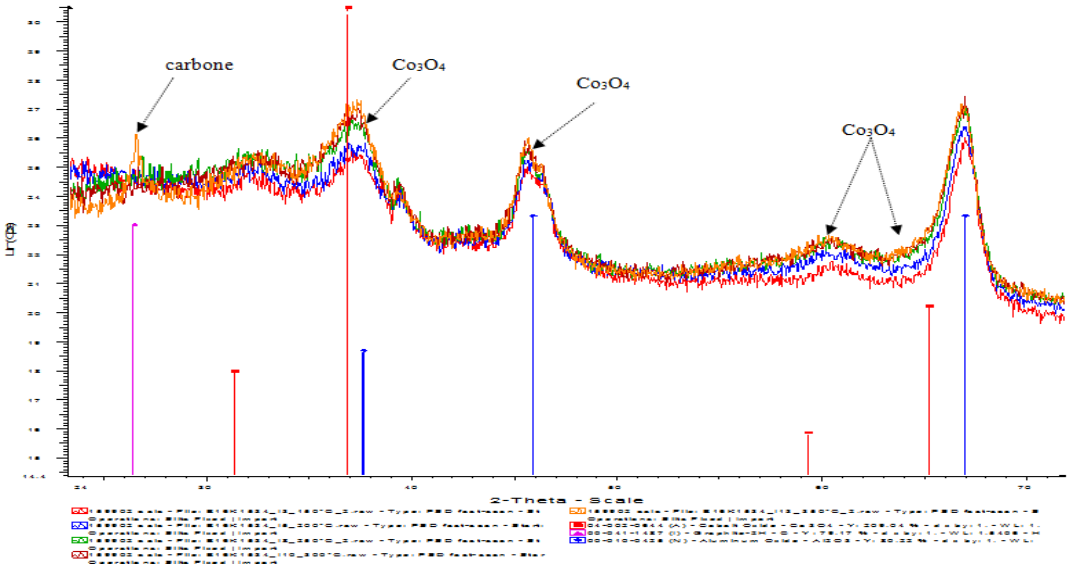

Figure 28 - XRD *'in-situ'* results for 150˚C (red), 200˚C (blue), 250˚C (green), 300˚C (brown) and 350˚C (orange).

Between 350˚C and 450˚C the signal of Co_3O_4 evolves, having always the presence of carbon. At the final temperature of 450˚C is detected the formation of cobalt aluminate. (Figure 29).

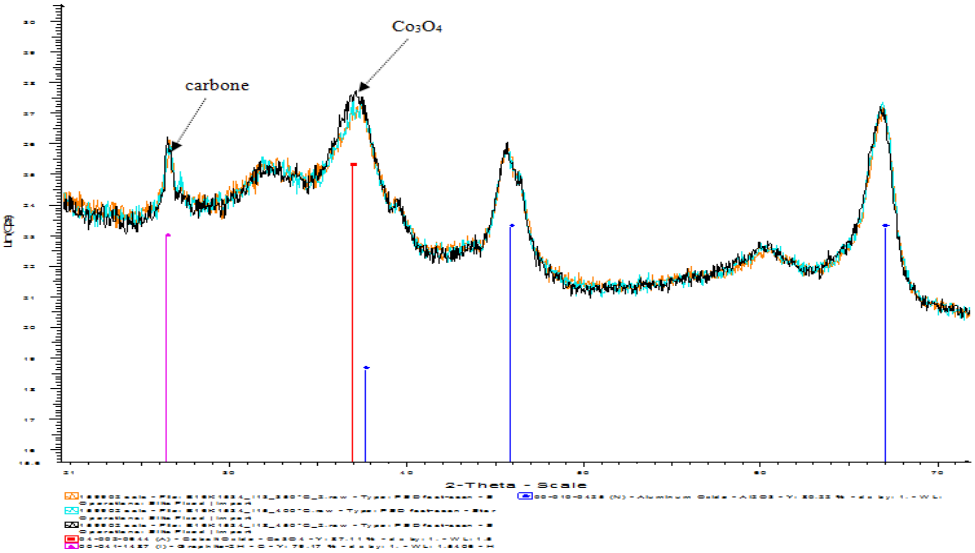

Figure 29 - XRD 'in-situ' results for 350˚C (orange), 400˚C (blue), 450˚C (black).

Thus, the results demonstrate that the problem in the calcination of cobalt catalysts is due to the formation of cobalt aluminate, at 450˚C.

According to the literature [44], TPR profiles show that for temperatures higher than 600°C occurs the formation of cobalt silicate or cobalt aluminate. The interaction between silica support and cobalt is weaker than in alumina supported catalysts, which leads to better cobalt reducibility. In

alumina supported catalysts, cobalt oxide strongly interacts with alumina, forming relatively small cobalt crystallites which may result in diffusion of cobalt active phase into alumina and formation of cobalt aluminate. Strong temperature elevations decreases not only the reducibility of the catalysts, but also the metallic dispersion due to the formation of cobalt aluminates [45]. In general, for calcination temperatures higher than 500°C, the cobalt reducibility decreases.

4.2 Arsenic trapping

To study the influence of the catalyst type and the variation of arsenic concentration with two different organo-arsenic compounds ($AsPh_3$ and $AsEt_3$), the adsorption reaction of arsenic mass trapping is assumed as a first order reaction due to be a traditional and simple way to treat the results, the objective of this work being not to determine the order of the reaction. Knowing this fact, it is possible to determine the kinetic constant:

$$r = k[C] \quad \text{Eq. 16}$$

$$r = -\frac{\Delta[C]}{\Delta t} \quad \text{Eq. 17}$$

$$\leftrightarrow k\Delta t = -\frac{1}{[C]}\Delta[C] \quad \text{Eq. 18}$$

Where,

k : Kinetic constant of the reaction

$[C]$: Concentration of the organo-arsenic coumpound

t : Time of reaction

Integrating this equation from the initial time, t=0, to a certain time, t=t, and from the initial concentration, $[C]_0$, to the concentration at t=t, $[C]$, it is possible to obtain:

$$k\int_0^t \Delta t = -\int_{[C]_0}^{[C]} \frac{1}{[C]}\Delta[C] \leftrightarrow ln[C] = ln[C]_0 - kt \quad \text{Eq. 19}$$

$$\leftrightarrow ln\left(\frac{[C]}{[C]_0}\right) = -kt \quad \text{Eq. 20}$$

Thus, the integrated equation results in a linear regression where $y = ln\left(\frac{[C]}{[C]_0}\right)$ and $x = t$, with $-k$ representing the slope.

The variation of concentration with time is given by the peak areas obtained by gas chromatography of the samples taken during the reaction and, in this way, it is possible to determine not only the conversion of the reaction but also the kinetic constant of the reaction.

4.2.1 Reference experiments with RC1 and RC2

Two commercial trapping mass available in large quantity have been used to develop a methodology for this study. RC2 catalysts contains nickel and RC1 is composed by nickel, cobalt and molybdenum, both on alumina support.

4.2.1.1 Effect of the nature and the concentration of Arsenic

For simplification, a model feed is used. The only arsenic components available are $AsMet_3$ (trimethylarsine), $AsEt_3$ and $AsPh_3$. For this work were selected $AsEt_3$ and $AsPh_3$ in order to study the reactivity of paraffinic and aromatic organo-arsenic compounds. Knowing the boiling range of gasoline (50-220˚C), $AsEt_3$ is within this range (bp = 140˚C), $AsMet_3$ is a little bit volatile (bp = 56˚C) and $AsPh_3$ has a boiling point much higher than the range of gasoline (bp = 373˚C) and cannot be found in the real gasoline, however was selected, as explained before, to study the reactivity of aromatic arsenic components.

4.2.1.1.1 Triphenylarsine ($AsPh_3$)

Four catalysts were tested in order to determine the arsenic mass trapping (conversion) for a feed containing $AsPh_3$.

An example of how it is determined the conversion and the kinetic constant is given for the RC1 catalyst with high concentration of $AsPh_3$ (2155 ppm As):

Table 10 - Variation of concentration with time for RC1 with high concentration of $AsPh_3$.

Reaction time, t (min)	$AsPh_3$ (Area Unit)	$\frac{[C]}{[C]_0}$	$ln\left(\frac{[C]}{[C]_0}\right)$
0	1176,10	1,00	0,00
5	1034,60	0,88	-0,13
10	904,50	0,77	-0,26
15	795,17	0,68	-0,39
20	692,27	0,59	-0,53
30	560,20	0,48	-0,74
40	464,47	0,39	-0,93
50	387,47	0,33	-1,11
60	334,10	0,28	-1,26
75	261,10	0,22	-1,51
90	198,60	0,17	-1,78
120	112,40	0,10	-2,35

The linear regression is given by:

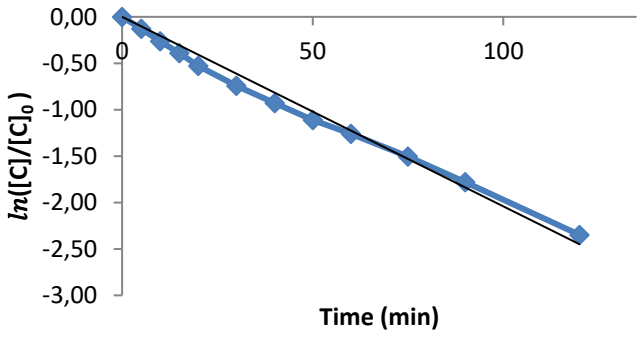

Figure 30 - Linear regression to obtain the kinetic constant.

$$y = -0.019x\ ;\ R^2 = 0.995 \qquad \text{Eq. 21}$$

By Equation 21 it is possible to determine the kinetic constant, from the value of the slope:

$$k\left(min^{-1}\right) = 0.019$$

Thus, with the value of $\frac{[C]_{120}}{[C]_0}$ the final conversion of arsenic for RC1 is $x = 0.90$.

For the remaining catalysts, the decrease in concentration versus time, the kinetic constant and the final conversion are summarized hereafter.

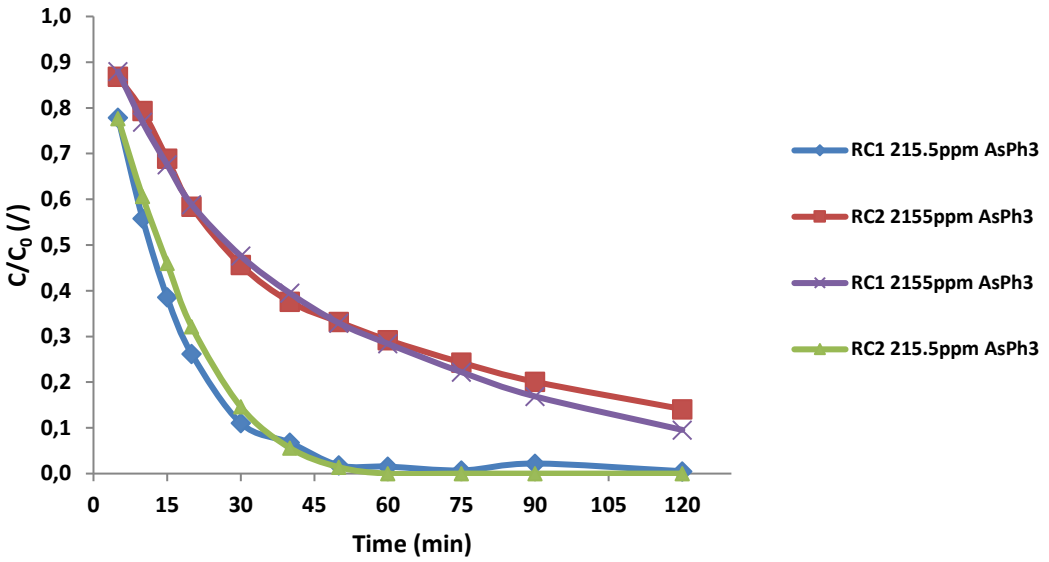

Figure 31 – Arsenic trapping of $AsPh_3$ for RC1 and RC2.

Due to the shape of the curves (Figure 31) it is possible to conclude that the kinetics do not correspond to a first order kinetic. However, as it was explained before, it is not the objective to determine the kinetics of arsenic adsorption.

Table 11 – Conversion rates and kinetic constants for RC1 and RC2.

Type of catalyst	Arsenic concentration (ppm)	Arsenic trapped (ppm)	k (min^{-1})	Conversion (%)
RC1	2155	1940	1.9×10^{-2}	90
	215.5	214	4.5×10^{-2}	99
RC2	2155	1854	1.6×10^{-2}	86
	215.5	215.5	8.7×10^{-2}	100

RC catalysts show high conversions, especially for low concentrations feeds of $AsPh_3$, and kinetics in the order of 10^{-2} min^{-1}.

4.2.1.1.2 Triethylarsine ($AsEt_3$)

Four catalysts were tested in order to determine the arsenic mass trapping (conversion) for a feed containing $AsEt_3$.

Proceeding in the same way, it is determined the conversion and the kinetic constant for the RC1 catalyst with high concentration of $AsEt_3$ (2155 ppm As):

Table 12 - Variation of concentration with time for RC1 with high concentration of $AsEt_3$.

Reaction time, t (min)	$AsEt_3$ (Area Unit)	$\frac{[C]}{[C]_0}$	$ln\left(\frac{[C]}{[C]_0}\right)$
0	475,67	1,00	0,00
5	446,93	0,94	-0,06
10	420,10	0,88	-0,12
15	414,93	0,87	-0,14
20	412,20	0,87	-0,14
30	405,90	0,85	-0,16
40	397,27	0,84	-0,18
50	380,40	0,80	-0,22
60	370,43	0,78	-0,25
75	347,03	0,73	-0,32
90	328,37	0,69	-0,37
120	289,77	0,61	-0,50

Treating the results presented in Table 12, the following linear regression is obtained:

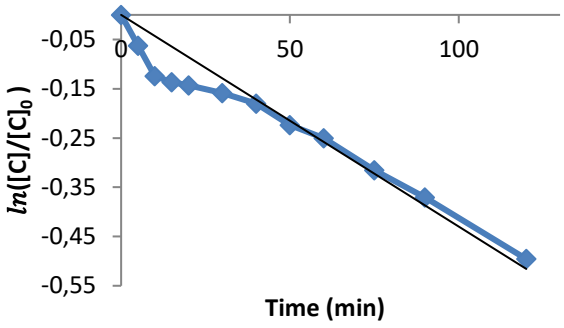

Figure 32 - Linear regression to obtain the kinetic constant.

$$y = -0.003x\ ;\ R^2 = 0.981 \qquad \text{Eq. 22}$$

By Equation 22 it is possible to determine the kinetic constant, from the value of the slope:

$$k\left(min^{-1}\right) = 0.003$$

The final conversion rate of mass trapping represents the total quantity of arsenic adsorbed in the catalyst. Doing a mass balance, the final content of arsenic in the liquid phase (corresponds to

$t = 120$ min) is known, and with the initial content of arsenic ($t = 0$ min), it is possible to calculate the final conversion as:

$$x = \frac{[C]_0 - [C]_{120}}{[C]_0} = 1 - \frac{[C]_{120}}{[C]_0} \qquad \text{Eq. 23}$$

Thus, with the value of $\frac{[C]_{120}}{[C]_0}$ the final conversion of arsenic for RC1 is $x = 0.39$.

For the remaining catalysts, the decrease in concentration versus time, the kinetic constant and the final conversion are summarized hereafter.

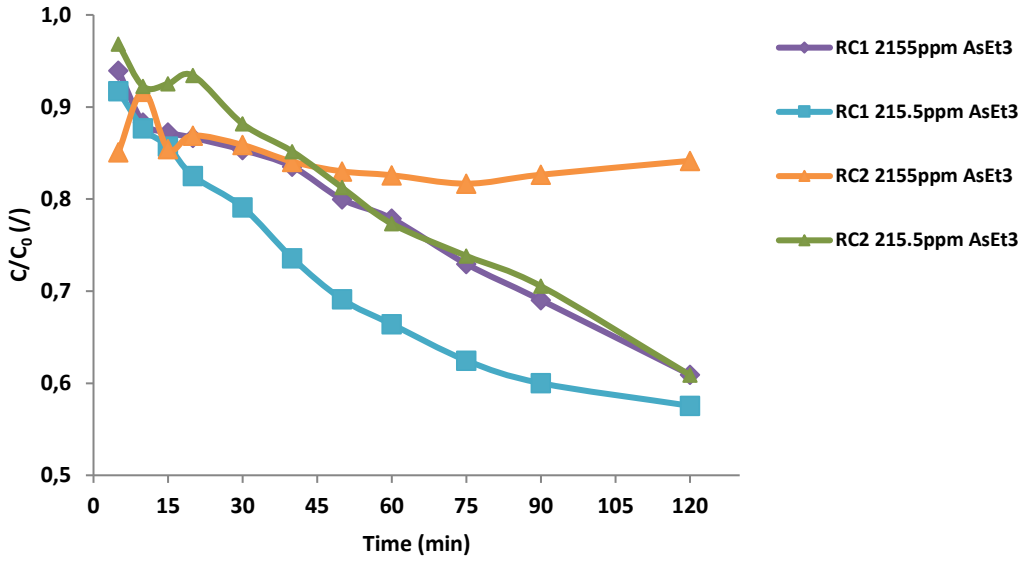

Figure 33 - Arsenic trapping of $AsEt_3$ for RC1 and RC2.

Table 13 - Conversion rates and kinetics constant for RC1 and RC2.

Type of catalyst	Arsenic concentration (ppm)	Arsenic trapped (ppm)	k (min^{-1})	Conversion (%)
RC1	2155	841	3×10^{-3}	39
	215.5	91	4×10^{-3}	42
RC2	2155	345	1×10^{-3}	16
	215.5	84	4×10^{-3}	39

For concentrated feeds of $AsEt_3$, RC catalysts have lower conversions compared with concentrated feeds of $AsPh_3$. The kinetics are also lower (k=10^{-3} min^{-1}).

4.2.1.2 Reproducibility of the catalytic tests with $AsPh_3$

In order to ensure the reproducibility of the tests, two tests have been duplicated for a concentrated feed of $AsPh_3$ (2155 ppm As). The graphics show very good results, as it is possible to verify in the following figures:

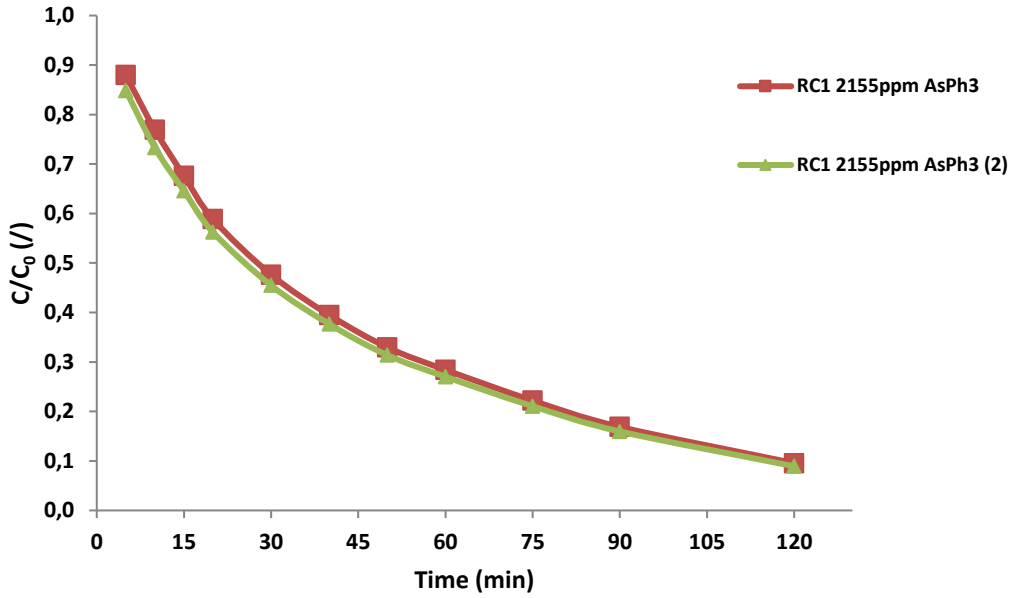

Figure 34 – Reproducibility of RC1 for high concentrations of $AsPh_3$.

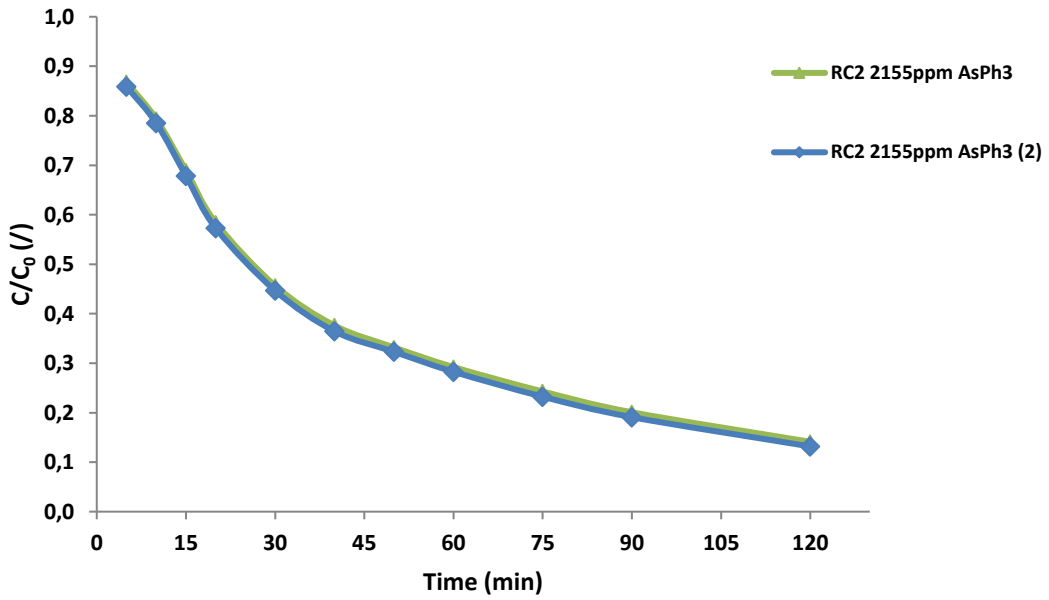

Figure 35 - Reproducibility of RC2 for high concentrations of $AsPh_3$.

4.2.1.3 Competition between desulfurization and dearsenification

To study the competition between the conversion for trapping arsenic and sulphur, two different catalysts were tested: RC2 and RC1.

Using toluene as solvent, a concentrated feed was prepared with low concentration of As, 215.5 ppm, in the form of $AsPh_3$ and with a concentration of 1000 ppm of sulphur, in the form of 3-methylthiophene.

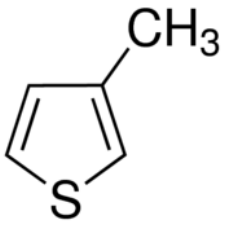

Form: liquid

Molecular Weight: 98.17 g/mol

Density: 1.02 g/cm^3

Melting Point: -69°C

Boiling Point: 115-117°C

Figure 36 – Properties of 3-methylthiophene **[46]**.

To determine the kinetic parameters are used the same equations explained in **chapter 4.2**.

In this way, it is possible to obtain the conversion and the kinetic constant for both compounds. The results are explained for RC2.

Table 14 - Variation of arsenic and sulphur concentration with time for RC2.

Reaction time, t (min)	$AsPh_3$ (Area Unit)	3 –Me–Thi (Area Unit)	$\left(\frac{[C]}{[C]_0}\right)_{As}$	$\left(\frac{[C]}{[C]_0}\right)_{S}$	$\left(ln\left(\frac{[C]}{[C]_0}\right)\right)_{As}$	$\left(ln\left(\frac{[C]}{[C]_0}\right)\right)_{S}$
0	135,12	420,04	1,00	1,00	0,00	0,00
5	109,47	422,47	0,81	1,01	-0,21	0,01
10	83,80	418,27	0,62	1,00	-0,48	0,00
15	62,53	415,73	0,46	0,99	-0,77	-0,01
20	44,37	407,27	0,33	0,97	-1,11	-0,03
30	21,57	396,47	0,16	0,94	-1,84	-0,06
40	10,17	391,67	0,08	0,93	-2,59	-0,07
50	4,57	375,17	0,03	0,89	-3,39	-0,11
60	2,00	359,90	0,01	0,86	-4,21	-0,15
75	0,00	354,27	0,00	0,84	n.d.	-0,17
90	0,00	341,27	0,00	0,81	n.d.	-0,21
120	0,00	314,80	0,00	0,75	n.d.	-0,29

For arsenic the linear regression is given by:

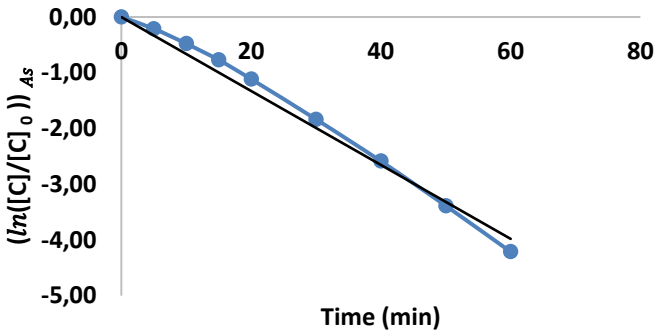

Figure 37 - Linear regression for arsenic to obtain the kinetic constant.

$$y = -0.073x\ ;\ R^2 = 0.997 \qquad \text{Eq. 24}$$

By Equation 24 it is possible to determine the kinetic constant, from the value of the slope:

$$k_{As}\ (min^{-1}) = 0.073$$

Thus, with the value of $\left(\frac{[C]_{120}}{[C]_0}\right)_{As}$ the final conversion of arsenic for RC2 is $x_{As} = 1$.

Proceeding in the same way it is possible to obtain the linear regression for sulphur:

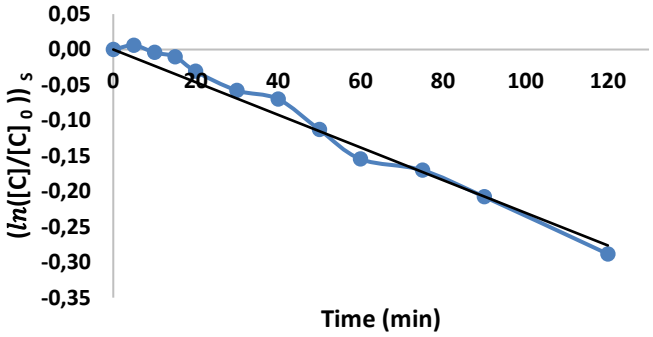

Figure 38 - Linear regression for sulphur to obtain the kinetic constant.

$$y = -0.003x\ ;\ R^2 = 0.993 \qquad \text{Eq. 21}$$

By Equation 25 it is possible to determine the kinetic constant, from the value of the slope:

$$k_S\ (min^{-1}) = 0.003$$

Thus, with the value of $\left(\frac{[C]_{120}}{[C]_0}\right)_S$ the final conversion of sulphur for RC2 is $x_S = 0.25$.

In order to determine the **selectivity of arsenic**, it is possible to relate the two kinetic constants:

$$S_{As/S} = \frac{k_{As}}{k_S} \qquad \text{Eq. 22}$$

Thus,

$$S_{As/S} = \frac{0.073}{0.003} = 28.2$$

This means that the mass trapping of arsenic is more efficient than the trapping of sulphur in around 28.2 times, wherein the reaction is favored for the side of arsenic trapping.

Then, the results for both catalysts are following summarized: the decrease in concentration versus time, the kinetic constants and the final conversions.

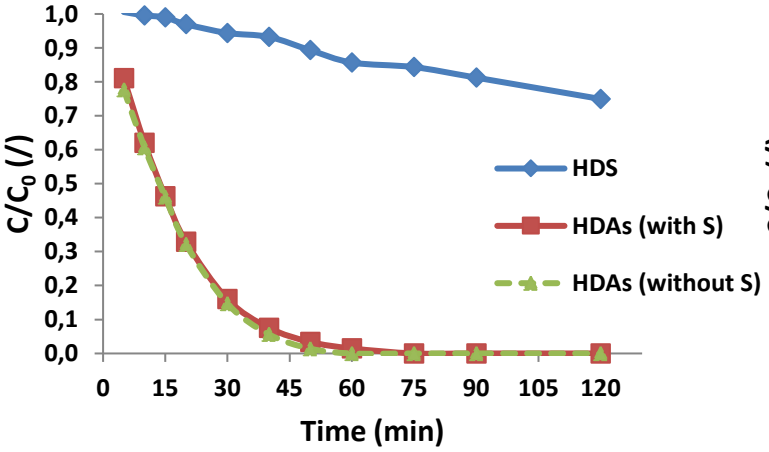

Figure 39 – Arsenic and sulphur trapping for RC2.

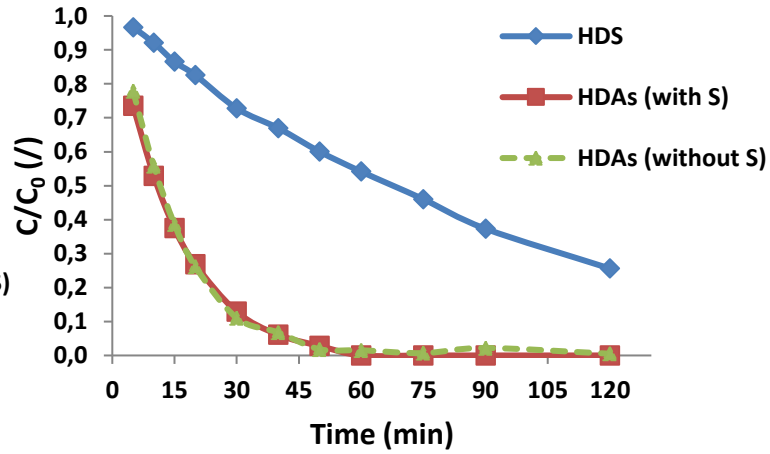

Figure 40 – Arsenic and sulphur trapping for RC1.

Table 15 - Arsenic and sulphur concentrations and amount of mass trapping.

Type of catalyst	Arsenic concentration (ppm)	Sulphur concentration (ppm)	Arsenic trapped (ppm)	Sulphur trapped (ppm)
RC2	215.5	1000	215.5	250
RC1	215.5	1000	215.5	250

Table 16 - Conversion rates, kinetic constants and selectivities for both catalysts.

Type of catalyst	k_{As} (min^{-1})	k_S (min^{-1})	$Conversion_{As}$ (%)	$Conversion_S$ (%)	$S_{As/S}$
RC2	7.3×10^{-2}	3.0×10^{-3}	100	25	28.2
RC1	7.3×10^{-2}	1.1×10^{-2}	100	74	6.4

Comparing the results for both catalysts it is possible to verify that RC1 and RC2 reach the total conversion for arsenic, however RC1 is more efficient to trap arsenic and sulphur at the same time. Knowing that the composition of RC2 is only nickel and that RC1 is composed by nickel, cobalt and molybdenum, it is possible to conclude that nickel is responsible for the arsenic trapping (as concluded previously) and the other metals play the role to increase the reaction of desulphurization. Nevertheless, nickel is also responsible for trap sulfur as can be seen in the conversion of this compound equal to 25% for RC2.

Following the curves of dearsenification without sulphur (represented by a dashed line) it is possible to conclude that the influence of sulphur to trap arsenic can be considered negligible for both catalysts in this concentration range.

4.2.2 Experiments with metals impregnated on alumina support

4.2.2.1 Effect of the nature and the concentration of Arsenic

4.2.2.1.1 Triphenylarsine ($AsPh_3$)

A catalyst impregnated with nickel and citric acid was tested in order to determine the arsenic mass trapping (conversion) for a feed containing $AsPh_3$.

Proceeding in the same way than the explained for the RC catalysts, it is obtained the decrease in concentration versus time, the conversion and the kinetic constant with high concentration of $AsPh_3$ (2155 ppm As):

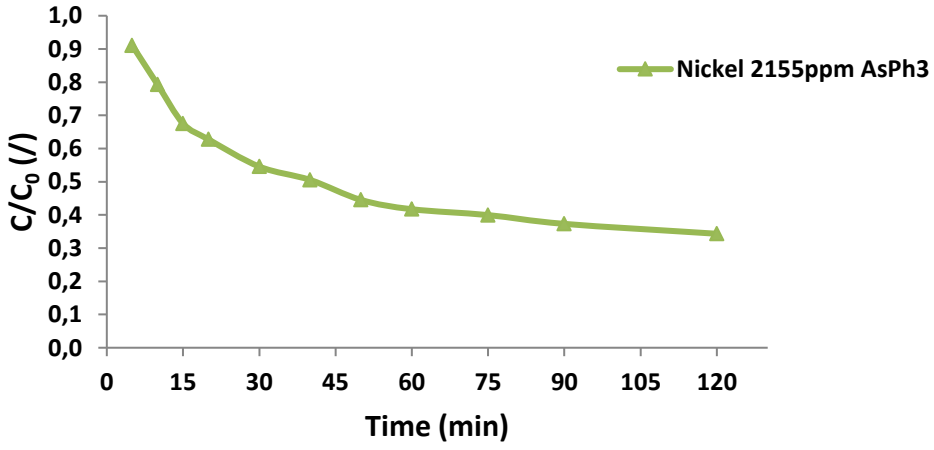

Figure 41 - Arsenic trapping of $AsPh_3$ for nickel catalyst.

Table 17 - Conversion rates and kinetics constant for nickel catalyst.

Type of catalyst	Arsenic concentration (ppm)	Arsenic trapped (ppm)	k (min^{-1})	Conversion (%)
Nickel on alumina+	2155	1423	8.0×10^{-3}	66

+ prepared with an aqueous solution with citric acid

The nickel catalyst on alumina support presents a high conversion of arsenic for $AsPh_3$ feed but lower than the RC catalysts.

4.2.2.1.2 Triethylarsine ($AsEt_3$)

Eight catalysts were tested in order to determine the arsenic mass trapping (conversion) for a feed containing $AsEt_3$.

The decrease in concentration versus time, the conversions and the kinetic constants are summarized hereafter:

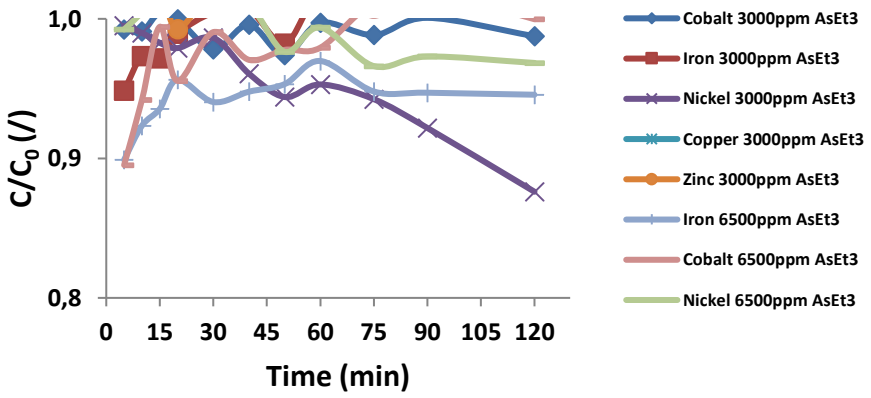

Figure 42 - Arsenic trapping of $AsEt_3$ for metals impregnated on alumina support.

Table 18 - Conversion rates and kinetics constant for metals impregnated on alumina support.

Type of catalyst	Arsenic concentration (ppm)	Arsenic trapped (ppm)	k (min^{-1})	Conversion (%)
Nickel on alumina	6500	195	4×10^{-4}	3
Cobalt on alumina	6500	0	0	0
Iron on alumina	6500	0	0	5
Nickel on alumina+	3000	360	1×10^{-3}	12
Cobalt on alumina+	3000	30	3×10^{-5}	1
Iron on alumina+	3000	0	0	0
Zinc on alumina+	3000	0	0	0
Copper on alumina+	3000	0	0	0

+ prepared with an aqueous solution with citric acid

Metals impregnated on alumina support show a very low conversion of $AsEt_3$ with low kinetics ($k\approx10^{-4}$ min^{-1}).

4.2.3 Experiments with metals impregnated on HDS catalyst

HDS catalysts contain molybdenum and it is important to study their influence with metals impregnated, in order to compare with the other types of catalysts.

4.2.3.1 Effect of the nature and the concentration of Arsenic

4.2.3.1.1 Triphenylarsine ($AsPh_3$)

Five catalysts were tested in order to determine the arsenic mass trapping (conversion) for a feed containing $AsPh_3$.

The decrease in concentration, the conversions and the kinetic constants are summarized hereafter:

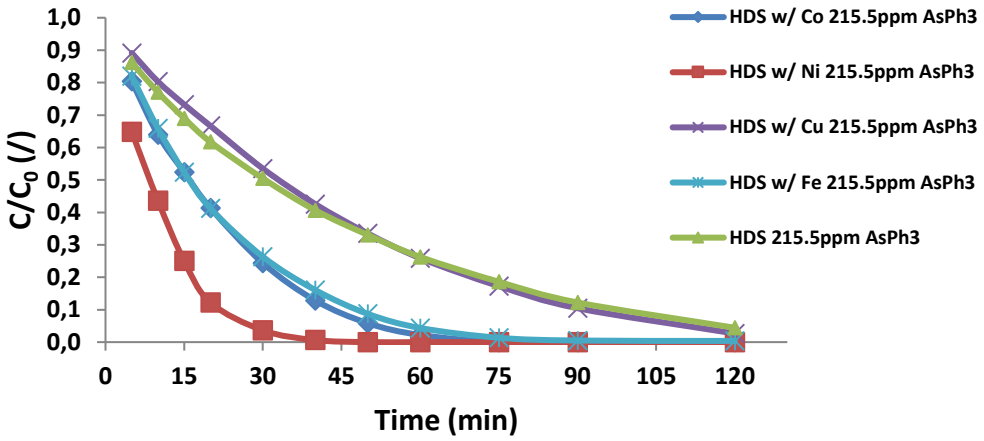

Figure 43 - Arsenic trapping of $AsPh_3$ for HDS catalysts.

Table 19 - Conversion rates and kinetics constant for HDS catalysts.

Type of catalyst	Arsenic concentration (ppm)	Arsenic trapped (ppm)	k (min^{-1})	Conversion (%)
HDS	215.5	207	2.5×10^{-2}	96
HDS + Cu^+	215.5	209	2.9×10^{-4}	97
HDS + Fe^+	215.5	215.5	5.3×10^{-4}	100
HDS + Ni^+	215.5	215.5	1.3×10^{-1}	100
HDS + Co^+	215.5	215.5	6.4×10^{-2}	100

+ prepared with an aqueous solution with citric acid

HDS catalysts have higher conversions for $AsPh_3$ feeds, similar to the ones observed for RC catalysts. However, the kinetics are different and nickel is responsible to improve this value ($k = 10^{-4/-2}$ min^{-1} to $k = 10^{-1}$ min^{-1}).

4.2.3.1.2 Triethylarsine ($AsEt_3$)

A HDS catalyst from *Axens* impregnated with nickel and citric acid was tested in order to determine the arsenic mass trapping (conversion) for a feed containing $AsEt_3$.

The decrease in concentration versus time, the conversions and the kinetic constants are summarized hereafter for high concentration of $AsEt_3$ (2155 ppm As):

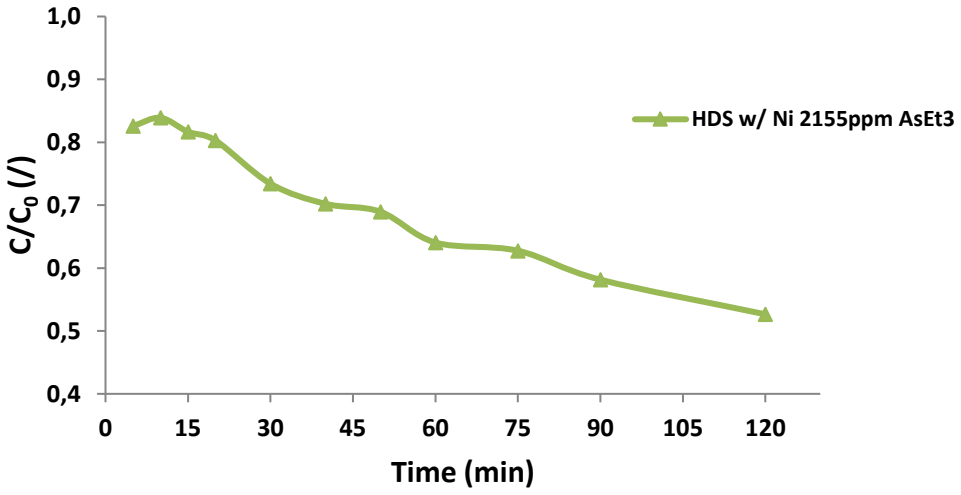

Figure 44 - Arsenic trapping of $AsEt_3$ for HDS catalyst impregnated with nickel.

Table 20 - Conversion rates and kinetics constant for HDS catalyst impregnated with nickel.

Type of catalyst	Arsenic concentration (ppm)	Arsenic trapped (ppm)	k (min^{-1})	Conversion (%)
HDS + Ni^+	2155	1013	4×10^{-3}	47

+ prepared with an aqueous solution with citric acid

HDS catalyst impregnated with nickel show higher conversions for $AsEt_3$ feed than the ones observed for the metals impregnated on alumina support and similar to the conversions for RC catalysts, in the same order of kinetics value ($k = 10^{-3}$ min^{-1}).

4.2.3.2 Trapping rate of $AsPh_3$

All of the HDS catalysts prepared have an arsenic trapping conversion for $AsPh_3$ around 100%, however the type of metallic precursor influences the time necessary to trap all the arsenic content.

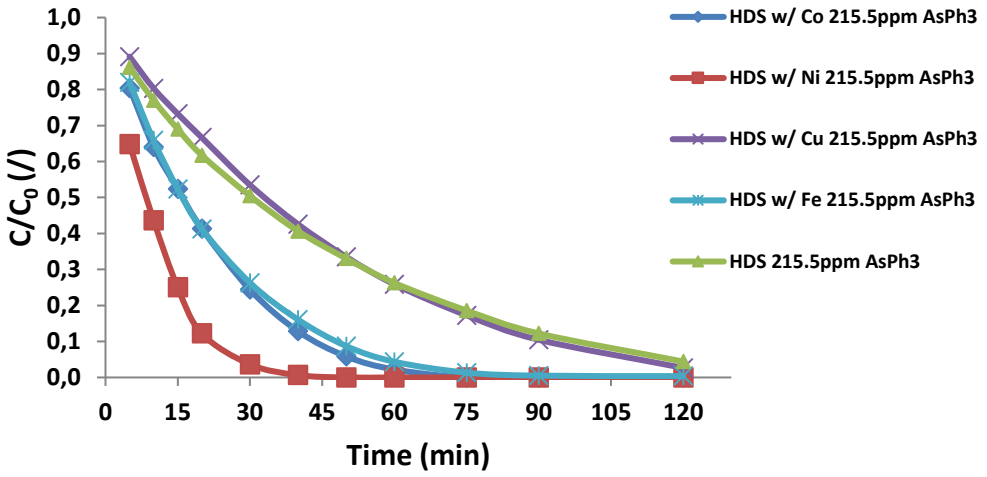

Figure 45 - Trapping speed for $AsPh_3$ with HDS catalysts.

Both the HDS catalyst with nickel such as the one with iron and cobalt have 100% conversion. The required times to reach the final conversion are presented in the following table as well as the kinetics constant for each catalyst.

Table 21 - Time required to trap all the arsenic content and kinetic constants.

Type of catalyst	Time required (min)	k (min^{-1})
HDS + Fe^+	90	5.3×10^{-4}
HDS + Co^+	75	6.4×10^{-2}
HDS + Ni^+	50	1.3×10^{-1}

+ prepared with an aqueous solution with citric acid

The time required to trap all the arsenic content is inversely proportional to the kinetic constant for each catalyst, in other words, the catalyst that shows a bigger kinetic constant has a shorter required time.

Thus, knowing that the composition of the HDS catalyst is cobalt and molybdenum, the presence of nickel precursor on this catalyst increases the efficiency of mass trapping, reaching the conversion of 100% in less time.

4.2.4 Influence of molybdenum in the efficiency of nickel catalysts for $AsEt_3$ and $AsPh_3$

According to the results obtained in the previous chapters, the catalysts that contain nickel in their composition have higher trapping conversions. Therefore, it is interesting to study the influence of molybdenum on these type of catalysts for a concentrated feed of $AsEt_3$ and $AsPh_3$.

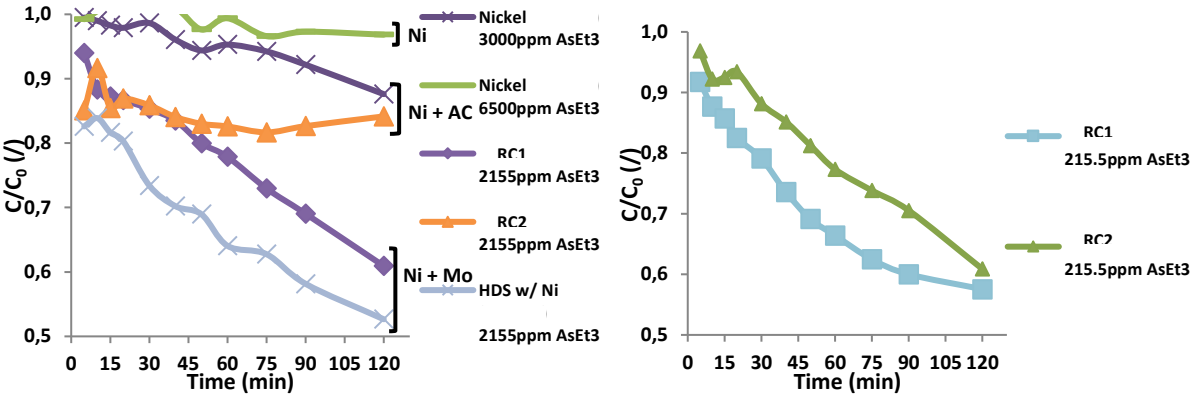

Figure 46 - Influence of molybdenum for high and low concentrations of $AsEt_3$.

Table 22 - Influence of molybdenum for high concentration of $AsEt_3$.

Type of catalyst	Conversion (%)
Ni	3
Ni + AC	14
Ni + Mo	43

Table 23 - Influence of molybdenum for low concentrations of $AsEt_3$.

Type of catalyst	Conversion (%)
Ni + AC	39
Ni + Mo	42

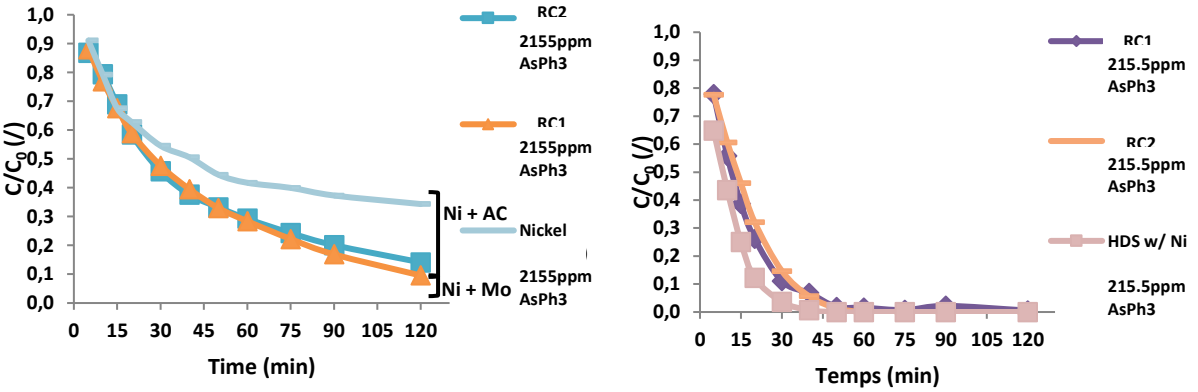

Figure 47 - Influence of molybdenum for high and low concentrations of $AsPh_3$.

Table 24 – Influence of molybdenum for high concentrations of $AsPh_3$.

Type of catalyst	Conversion (%)
Ni + AC	76
Ni + Mo	90

Table 25 - Influence of molybdenum for low concentrations of $AsPh_3$.

Type of catalyst	Conversion (%)
Ni + AC	100
Ni + Mo	100

For both forms of concentrated feeds the influence of molybdenum is most pronounced for high concentrations of arsenic. For $AsEt_3$, the presence of molybdenum increases the conversion in around fifteen times in relation to the nickel catalyst and three times regarding the nickel catalyst prepared with citric acid (Table 22). For $AsPh_3$, the value of conversion increases 1.2 times in relation to the one prepared with citric acid (Table 25).

For low concentration values, the influence of molybdenum for both feeds appears to be negligible.

Thus, molybdenum affects the trapping mass of high concentrated organo-arsenic compounds, especially $AsEt_3$.

4.2.5 Comparison between all the catalysts

As shown before in **chapter 4.2.1**, **4.2.2** and **4.2.3**, in all the cases the conversions are higher for a concentrated feed of $AsPh_3$. To compare better the mass trapping of organo-arsenic compounds, the conversions and the kinetic constants are summarized hereafter for $AsPh_3$ and $AsEt_3$:

Table 26 - Conversion rates and kinetics constant for $AsPh_3$ feed.

Type of catalyst	Arsenic concentration (ppm)	Arsenic trapped (ppm)	k (min^{-1})	Conversion (%)
Nickel on alumina$^+$	2155	1423	8.0×10^{-3}	66
RC1	2155	1940	1.9×10^{-2}	90
	215.5	214	4.5×10^{-2}	99
RC2	2155	1854	1.6×10^{-2}	86
	215.5	215.5	8.7×10^{-2}	100
HDS	215.5	207	2.5×10^{-2}	96
HDS + Cu$^+$	215.5	209	2.9×10^{-4}	97
HDS + Fe$^+$	215.5	215.5	5.3×10^{-4}	100
HDS + Ni$^+$	215.5	215.5	1.3×10^{-1}	100
HDS + Co$^+$	215.5	215.5	6.4×10^{-2}	100

+ prepared with an aqueous solution with citric acid

As can be seen in Table 26, the catalyst that shows a higher conversion even for low and high concentration of arsenic is RC1 (90% for high concentration and 99% for low concentration), composed by nickel, cobalt and molybdenum. The impregnation of metal precursors on HDS catalyst (composed by cobalt and molybdenum), increases the trapping conversion from 96% (for HDS without impregnated metals) to around 100%.

Comparing the nickel catalyst on alumina with the RC1 and HDS catalysts, it is possible to conclude that the presence of molybdenum on the catalyst composition leads to higher trapping conversion rates.

Table 27 - Conversion rates and kinetics constant for $AsEt_3$ feed.

Type of catalyst	Arsenic concentration (ppm)	Arsenic trapped (ppm)	k (min^{-1})	Conversion (%)
Nickel on alumina	6500	195	4×10^{-4}	3
Cobalt on alumina	6500	0	0	0
Iron on alumina	6500	0	0	5
Nickel on alumina+	3000	360	1×10^{-3}	12
Cobalt on alumina+	3000	30	3×10^{-5}	1
Iron on alumina+	3000	0	0	0
Zinc on alumina+	3000	0	0	0
Copper on alumina+	3000	0	0	0
RC1	2155	841	3×10^{-3}	39
	215.5	91	4×10^{-3}	42
RC2	2155	345	1×10^{-3}	16
	215.5	84	4×10^{-3}	39
HDS + Ni+	2155	1013	4×10^{-3}	47

+ prepared with an aqueous solution with citric acid

As can be seen in Table 27, the catalyst that shows a higher conversion even for low and high concentration of arsenic is RC1 (39% for high concentration and 42% for low concentration).

The HDS catalyst, prepared with an aqueous solution of nickel nitrate and citric acid, has the higher conversion for high concentration of arsenic, with around 47%.

Analyzing all the results, it is possible to conclude that the presence of nickel on the catalyst composition and the use of citric acid during the step of impregnation leads to higher trapping conversion rates, due to the increase of metal dispersion.

Thus, the dispersion agent and the nickel metallic promotor are responsible for a better arsenic mass trapping.

For both feeds, the conversions are higher for low concentrations of arsenic. It can be explained by the excess of metal compared with the amount of arsenic, due to that all the active sites are more available resulting in a higher and more rapid conversion.

4.3 Catalysts analysis

The catalysts which demonstrate higher conversions of mass trapping, for $AsPh_3$ and $AsEt_3$, were submitted to X-Ray Fluorescence analysis to discover the total arsenic content in the solid.

The results give the mass percentage of arsenic in relation to the total mass of the catalyst submitted to analysis. In order to relate this percentage with the mass of catalyst used in the reaction, the following deductions were made:

$$As\ (\%) = \left(\frac{m_{As}}{m_{As}+m_{catalyst}}\right) \times 100 \leftrightarrow \frac{1}{As} = 1 + \frac{m_{catalyst}}{m_{As}} \leftrightarrow \frac{m_{catalyst}}{m_{As}} = \frac{1-As}{As} \quad \text{Eq. 27}$$

Defining,

$$y = \frac{m_{As}}{m_{catalyst}} = \frac{As}{1-As} \quad \text{Eq. 28}$$

With,

$$Y\ (\%) = 100 \times y = 100 \times \frac{As}{1-As} \quad \text{Eq. 29}$$

Result,

$$Y\ (\%) = \frac{As\ (\%)}{1-\frac{As\ (\%)}{100}} \quad \text{Eq. 30}$$

Knowing the value of this ratio it is possible to determine the arsenic trapped on the catalyst after reaction assuming that $m_{catalyst}$ = 3 g and $V_{solvent}$ = 250 mL (toluene), according to the following equation:

$$As_{trapped}\ (ppm) = \frac{As_{catalyst}\ (mg)}{\rho_{toluene}(kg/L) \times V_{toluene}(L)} \quad \text{Eq. 31}$$

The results are presented in Table 28.

Table 28 – XRF results.

Type of catalyst	Arsenic concentration / compound (ppm)	As (wt. %)	Y (%)	As Trapped (g)*	Arsenic Trapped (ppm)
RC1	215.5 / $AsPh_3$	1.31	1.33	0.04	184
	2155 / $AsPh_3$	9.25	10.19	0.31	1411
	215.5 / $AsEt_3$	1.37	1.39	0.04	192
	2155 / $AsEt_3$	4.09	4.26	0.13	590
RC2	215.5 / $AsPh_3$	1.47	1.49	0.04	206
	2155 / $AsPh_3$	9.25	10.19	0.31	1411
	215.5 / $AsEt_3$	0.87	0.88	0.03	121
	2155 / $AsEt_3$	1.41	1.43	0.04	198
Nickel on alumina+	2155 / $AsPh_3$	8.19	8.92	0.27	1235
HDS	215.5 / $AsPh_3$	1.30	1.32	0.04	182
HDS + Cu+	215.5 / $AsPh_3$	1.29	1.31	0.04	181
HDS + Fe+	215.5 / $AsPh_3$	1.24	1.26	0.04	174
HDS + Ni+	215.5 / $AsPh_3$	1.35	1.37	0.04	189
	2155 / $AsEt_3$	5.09	5.36	0.16	742
HDS + Co+	215.5 / $AsPh_3$	1.29	1.31	0.04	181

* for 3 g of catalyst

+ prepared with an aqueous solution with citric acid

To compare this values with the ones given by gas chromatography a summary is presented in the following table.

Table 29 - Comparison between XRF and GC results.

Type of catalyst	Arsenic concentration / compound (ppm)	Arsenic Trapped (ppm)	Arsenic Trapped by GC (ppm)	Conversion by XRF (%)	Conversion by GC (%)	Variation (%)
RC1	215.5 / $AsPh_3$	184	214	85	99	16
	2155 / $AsPh_3$	1411	1940	65	90	38
	215.5 / $AsEt_3$	192	91	89	42	-53
	2155 / $AsEt_3$	590	841	27	39	42
RC2	215.5 / $AsPh_3$	206	215,5	96	100	4
	2155 / $AsPh_3$	1411	1854	65	86	31
	215.5 / $AsEt_3$	121	84	56	39	-30,8
	2155 / $AsEt_3$	198	345	9	16	74,3
Nickel on alumina+	2155 / $AsPh_3$	1235	1423	57	66	15,3
HDS	215.5 / $AsPh_3$	182	207	85	96	13,5
HDS + Cu+	215.5 / $AsPh_3$	181	209	84	97	15,5
HDS + Fe+	215.5 / $AsPh_3$	174	215,5	81	100	24,0
HDS + Ni+	215.5 / $AsPh_3$	189	215,5	88	100	13,8
	2155 / $AsEt_3$	742	1013	34	47	36,5
HDS + Co+	215.5 / $AsPh_3$	181	215,5	84	100	19,1

+ prepared with an aqueous solution with citric acid

Generally, the conversions observed by X-Ray Fluorescence are lower than the ones by Gas Chromatography, except for low concentrations of arsenic in the form of triethylarsine.

It can be explained by the fact that, for GC, the conversions are obtained knowing the arsenic concentration in the liquid before and after reaction, assuming that the difference in these values is the arsenic trapped on the catalyst. Thus, with the values obtained by XRF, it is a possible explanation that some arsenic during the reaction is in gas form, probably in the form of arsine (AsH_3).

Analysis of the total arsenic content of the liquid recovered at the end of the reaction are in progress. The results obtained have to be compared with the chromatographic ones.

Same analysis are also done with GC-MS (coupling Gas Chromatography with Mass Spectrometry), in order to identify if some arsenic containing compounds are formed (like $HAs\phi_2$, $H_2As\phi$, $HAsEt_2$, H_2AsEt, …).

5 Conclusions and future work

The aim of this work was to study the solids efficiency to trap organo-arsenic compounds. For that purpose, catalyst preparation methods were applied, by dry impregnation using different metal precursors on two supports (AAS and HDS catalyst) and thermal treatments (calcination). By Nitrogen Adsorption-desorption, it was possible to obtain the values for the specific surface area and porous volume and to conclude that are typical values for the commercial alumina AAS (125 m^2/g and 0.57 cm^3/g, respectively). The use of the dispersion agent during the impregnation increases the specific surface area for nickel catalysts as well as the total porous volume (24% and 8%, respectively). Mercury Porosimetry results show that the pores can be considered as mesopores (3,5-50 nm) and the use of the dispersion agent increases the pore volume of the catalysts in around 18%. X-Ray Diffraction was performed in order to determine the crystal size of the metal oxides and X-Ray Fluorescence to obtain the metal contents. To activate the catalysts, sulphurization was done with an excess of H_2S comparatively with the amount of metal present in the catalysts, to ensure that the sulphurization was complete.

Catalytic tests were performed in a Grignard reactor at 250˚C and 35 bar of hydrogen pressure, in order to determine the conversion of the dearsenification reaction and the kinetics of As mass trapping. The metal catalysts prepared and some catalysts from *Axens* (RC1 and RC2) were tested, using a model feed composed by toluene as solvent and two different natures of organo-arsenic concentrated feeds: triethylarsine and triphenylarsine. For all the tests done, the conversions are higher for a concentrated feed of $AsPh_3$. The catalyst that shows a higher conversion even for low and high concentrations of arsenic (for both types of feeds) is RC1, composed by nickel, cobalt and molybdenum (with 90% and 39% for high concentrations of $AsPh_3$ and $AsEt_3$, respectively, and 99% and 42% for low concentrations of $AsPh_3$ and $AsEt_3$, respectively). For RC catalysts was analyzed the reproducibility of the tests and the results demonstrate very good results. The mass trapping of this feeds increases with the dispersion of the metal on the catalyst. In general, the conversions are 2 times higher for $AsPh_3$ and Nickel is the most efficient metal precursor to trap both feeds, presenting conversions of 47% for $AsEt_3$ and 100% for $AsPh_3$ and kinetic constants of 4.0×10^{-3} min^{-1} and 1.3×10^{-1} min^{-1}, respectively. Even for other metals, with low concentrations of arsenic (215.5 ppm) in form of $AsPh_3$ the conversions are 100% but the trapping rate are higher for nickel (k = 1.3×10^{-1} min^{-1}) followed by cobalt (k = 6.4×10^{-2} min^{-1}) and iron (k = 5.3×10^{-4} min^{-1}). With these values it is possible to conclude that for both feeds the conversions are higher for low concentrations of arsenic. A possible explanation for these results is the excess of metal on the catalysts compared with the total amount of arsenic present in the concentrated feed. Due to that, all the active sites are more available to trap

arsenic, resulting in a higher and more rapid conversion. The presence of molybdenum on the catalysts increases the conversions for high concentrations of arsenic (2155 ppm) in 3 times, especially for a concentrated feed of $AsEt_3$.

Tests with a concentrated feed of arsenic ($AsPh_3$) and sulphur (3-Me-Thi) were performed with RC catalysts, with a relative concentration similar to the observed in a real gasoline, proving that RC1 is more efficient to trap arsenic and sulphur at the same time. The conversion for arsenic is higher than for sulphur, 100% and 75% respectively, with a selectivity for arsenic of 6.4. It is also possible to conclude that nickel is more responsible to promote the reaction of dearsenification, as concluded with the previous catalytic tests, and cobalt and molybdenum to increase the reactions of desulphurization. Comparing the dearsenification reaction with and without sulphur for RC catalysts, the presence of this compound can be considered insignificant in the concentration range used. However, it is not possible to ensure that these results have the same trends than for the real gasoline.

Regarding the perspectives of this work, six important points should be studied:

- Test HDS catalysts with $AsEt_3$: the HDS catalysts showed similar conversions observed for the ACT catalysts with a concentrated feed of $AsPh_3$. Thus, it is interesting to discover if this type of catalysts have similar conversions for a concentrated feed of $AsEt_3$;
- Change the experimental conditions of the reactor for a $AsEt_3$ feed: modifying the temperature and pressure of the reaction, increasing this value, may lead to higher conversions of arsenic;
- Perform catalytic tests with 3-Me-Thi using RC catalysts: determine the conversion of sulphur and compare with the value obtained for a concentrated feed constituted by an organo-arsenic compound and sulphur, in order to study the influence of arsenic in the reaction of desulphurization;
- Perform competition tests of dearsenification and desulphurization with HDS catalysts: as explained in the first topic, it is interesting to compare the conversions, kinetics and selectivity between RC and HDS catalysts;
- Test the competitivity of $AsEt_3$ and 3-Me-Thi: the competition between $AsPh_3$ and 3-Me-Thi was studied and it is important to compare these results but with a feed composed by $AsEt_3$;
- Do the same catalytic tests but with a feed composed by an olefin, an organo-arsenic compound ($AsPh_3$ and $AsEt_3$) and sulphur (3-Me-Thi): study the competition between all these compounds, determining the conversions, kinetics and selectivity of each compound;

6 References

[1] N. Courses, *Catalytic Cracking: Fluid Catalytic Cracking and Hydrocracking,* Lecture 5 - Module VI, 2013.

[2] F. Ribeiro, Catalytic Reforming - Petroleum Refining, Lisboa: Técnico Lisboa, 2014/2015.

[3] F. Ribeiro, FCC Process - Petroleum Refining, Lisboa: Instituto Superior Técnico, 2015.

[4] J. Siegel and C. Olsen, "Feed Contaminants in Hydroprocessing Units," *Advanced Refining Technologies Catalagrm 104 Special Edition,* 2008.

[5] F. Ribeiro, Hydroprocessing Units - Petroleum Refining, Lisboa: Instituto Superior Técnico, 2014.

[6] J. Jechura, *Hydroprocessing: Hydrotreating & Hydrocracking Chapters 7 & 9,* Colorado School of Mines, 2016.

[7] B. W.Hoffer, A. van Langeveld, J.-P. Janssens, R. L. C. Bonné, C. M. Lok and J. A. Moulijn, "Stability of Highly Dispersed Ni/Al2O3 Catalysts: Effects of Pretreatment," *Journal of Catalysis 192,* pp. 432-440, 2000.

[8] J.-P. Janssens, A. van Langeveld, R. L. C. Bonné, C. M. Lok and J. A. Moulijn, "Hydrotreating Technology for Pollution Control," New York, 1996.

[9] K. H. Bourne, P. P. Holmes and R. C. Pitkethly, "Proceedings 3rd International Congress on Catalysis Amsterdam 1964," New York, 1965.

[10] E. K. Poels, W. P. van Beek, W. Denhoed and C. Visser, "Fuel 1800," 1965.

[11] R. N. Merryfield, L. E. Gardner and G. D. Parks, "Arsenic Poisoning of Hydrodesulfurization Catalysts," *American Chemical Society,* 1985.

[12] A. Puig-Molina, L. P. Nielsen, A. M. Molenbroek and K. Herbst, "In Situ EXAFS study on the chemical state of arsenic deposited on a NiMoP/Al2O3 hydrotreating catalyst," *Catalysis Letters,* vol. 92, 2004.

[13] E. Furimsky and F. Massoth, "Catal. Today 52," 1999.

[14] P. Sarrazin, C. J. Cameron, Y. Barthel and M. E. Morrison, "Oil Gas J.," 1993.

[15] Y. A. Ryndin, J. Candy, B. Didillon, L. Savary and J. M. Basset, "J. Catal.," *198,* 2001.

[16] V. Maurice, Y. Ryndin, G. Bergeret, L. Savary, J. P. Candy and J. M. Basset, "J. Catal.," *204,* 2001.

[17] B. Nielsen and J. Villadsen, "Appl. Catal.," *11,* 1984.

[18] O. K. Bhan, "Arsenic removal catalyst and process for making same," *United States Patent 6.759.364,* 2004.

[19] J. B. Stigter, H. P. M. de Haan, R. Guicherit, C. P. A. Dekkers and M. L. Daane, "Environ. Pollut.," *451,* p. 107, 2000.

[20] S. Yang, J. Adjaye, W. C. McCaffrey and A. E. Nelson, "Density-functional theory (DFT) study of arsenic poisoning of NiMoS," *Journal of Molecular Catalysis A: Chemical 321,* pp. 83-91, 2010.

[21] Y. A. Ryndin, J. P. Candy, B. Didillon, L. Savary and J. M. Basset, "Surface Organometallic Chemistry on Metals Applied to the Environment: Hydrogenolysis of AsPh3 with Nickel Supported on Alumina," *Journal of Catalysis 198,* pp. 103-108, 2001.

[22] V. Maurice, Y. A. Ryndin, G. Bergeret, L. Savary, J. P. Candy and J. M. Basset, "Influence of the Dispersion of Metallic Particles on the Reaction of Triphenylarsine with Alumina-Supported Nickel," *Journal of Catalysis 204,* pp. 192-199, 2001.

[23] J. P. Candy, B. Didillon, F. L. ,. S. T. B. Smith and J. M. Basset, *J. Mol. Catal. 86,* p. 179, 1994.

[24] A. V. Cugini, D. V. Martello, D. Krastman, J. P. Baltrus, M. V. Ciocco, E. F. Frommell and G. D. Holder, The Effect of Catalyst Dispersion on the Activity of Unsupported Molybdenum Catalysts, University of Pittsburgh, Department of Chemical and Petroleum Engineering.

[25] X. Zhu, H.-r. Cho, M. Pasupong and J. R. Regalbuto, "Charge-Enhanced Dry Impregnation: A Simple Way to Improve the Preparation of Supported Metal Catalysts," *ACS Catalysis,* 2013.

[26] J. W. Geus and J. V. Dillen, "Handbook of Heterogeneous Catalysis," *John Willey and Sons,* vol. II, pp. 428-467, 1997.

[27] J. A. Schwarz, C. Contescu and A. Contescu, "Methods for Preparation of Catalytic Materials," *Chem. Rev,* pp. 477-510, 1995.

[28] A. V. Neimark, L. I. Kheifez and V. B. Fenelonov, "Ind. Eng. Chem. Prod. Res. Dev.," *439,* 1981.

[29] M. S. Heise and J. A. Schwarz, "Colloid Interface Sei.," *52,* 1988.

[30] M. S. Heise and J. A. Schwarz, "In Preparation of Catalysts IV.," *Eds. Stud. Surf. Sci. Catal. 1,* 1987.

[31] K. E. Coulter and A. G. Sault, *Journal of Catalysis, no. 154,* pp. 56-64, 1995.

[32] J. L. Figueiredo and F. R. Ribeiro, Catalise Heterogénea, 2ed., Lisboa: Fundaçao Calouste Gulbenkian, 2007.

[33] Y. Cesteros, P. Salagre, F. Medina and J. E. Sueiras, "Simple Synthesis and Characterization of Several Nickel Catalyst Precursors," *Journal of Chemical Education,* vol. 79, 2002.

[34] A. V. Pashigreva, G. A. Bukhtiyarova, O. V. Klimov, Y. A. Chesalov, G. S. Litvak and A. S. Noskov, "Activity and sulfidation behavior of the CoMo/Al2O3 hydrotreating catalyst: The effect of drying conditions," *Catalysis Today 149,* pp. 19-27, 2010.

[35] S. Texier, G. Berhault, G. Perot, V. Harle and F. Diehl, J. Catal. 223, 2004.

[36] L. Medici and R. Prins, J. Catal. 163, 1996.

[37] "Aqueous solubility of inorganic compounds at various temperatures," *CRC Handbook of Chemistry and Physics,* p. section 8, 2005.

[38] B. Müller, A. D. van Langeveld, J. A. Moulijn and H. Knözinger, "Characterization of Sulfided Mo/Al2O3 Catalysts by Temperature-Programmed Reduction and Low-Temperature Fourier Transform Infrared Spectroscopy of Adsorbed Carbon Monoxide," *J. Phys. Chem, 97,* pp. 9028-9033, 1993.

[39] A. Y. Khodakov, W. Chu and P. Fongarland, *Chemical Reviews 5,* vol. 107, pp. 1692-1744, 2007.

[40] K. S. W. Sing, "Physisorption of Nitrogen by Porous Materials," *Journal of Porous Materials,* pp. 5-8, 1995.

[41] J. Lynch, Physico-Chemical Analysis of Industrial Catalysts - A Pratical Guide to Characterization, Paris: Editions TECHNIP, 2004.

[42] D. P. Petru and L. Kempinski, *Catalysis Letters no. 1,* vol. 73, pp. 41-46, 2001.

[43] A. Lapidus, A. Krylova, J. Rathousky, A. Zukal and M. Jancalkova, *Applied Catalysis A: General, no. 80,* pp. 1-11, 1992.

[44] "Sigma-Aldrich," [Online]. Available: http://www.sigmaaldrich.com/catalog/product/aldrich/t81906?lang=fr&region=FR&gclid=CJqb5Oy-i80CFYu6GwodiTYOOQ. [Accessed 03 June 2016].

[45] "ChemicalBook," [Online]. Available: http://www.chemicalbook.com/ChemicalProductProperty_EN_CB4481924.htm. [Accessed 03 June 2016].

[46] "A. Aesar," [Online]. Available: https://www.alfa.com/pt/catalog/A13394/. [Accessed 01 August 2016].

This page was intentionally left blank

7 Appendix

Appendix I – Characterization Methods

N_2 adsorption-desorption

Three examples of this type of analysis are given for metals supported on alumina and HDS catalyst:

- For Nickel impregnated on alumina:

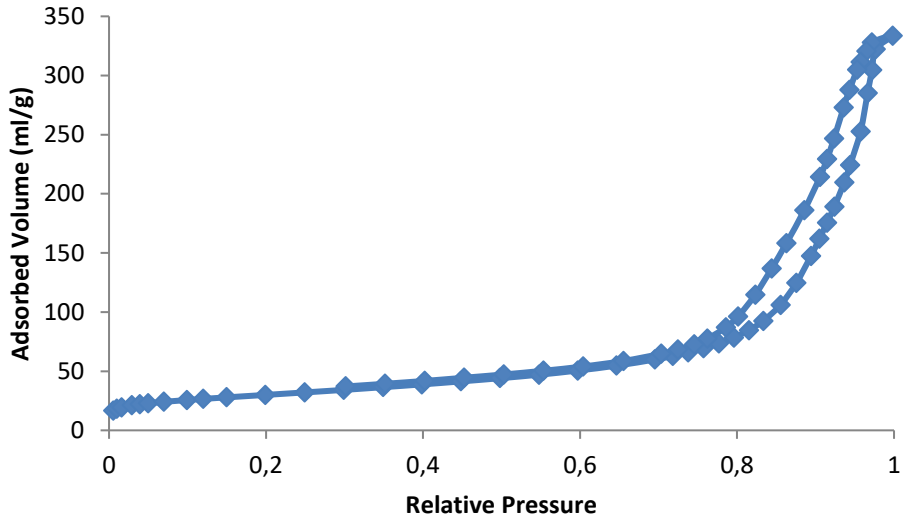

Figure I. 1 – Nitrogen adsorption-desorption isotherm.

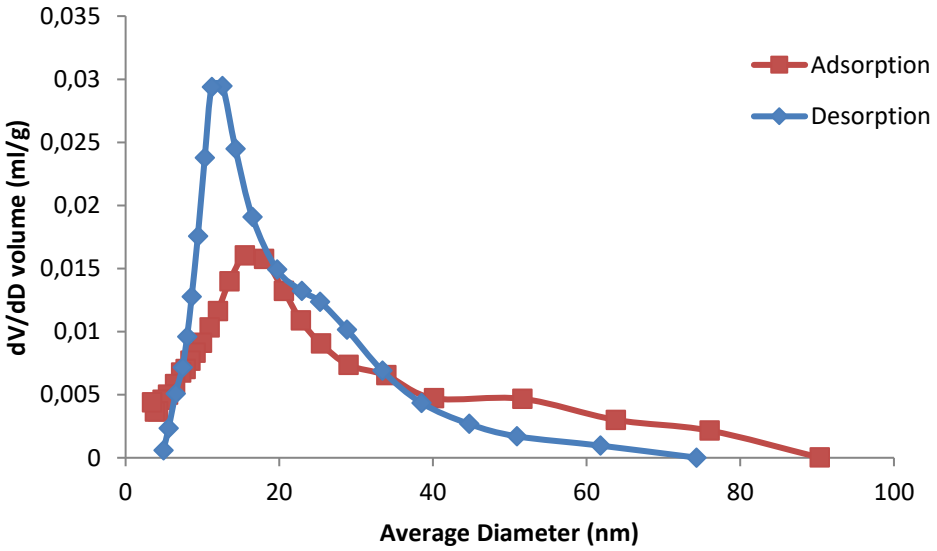

Figure I. 2 - BJH adsorption and desorption.

- For Nickel impregnated with citric acid on alumina:

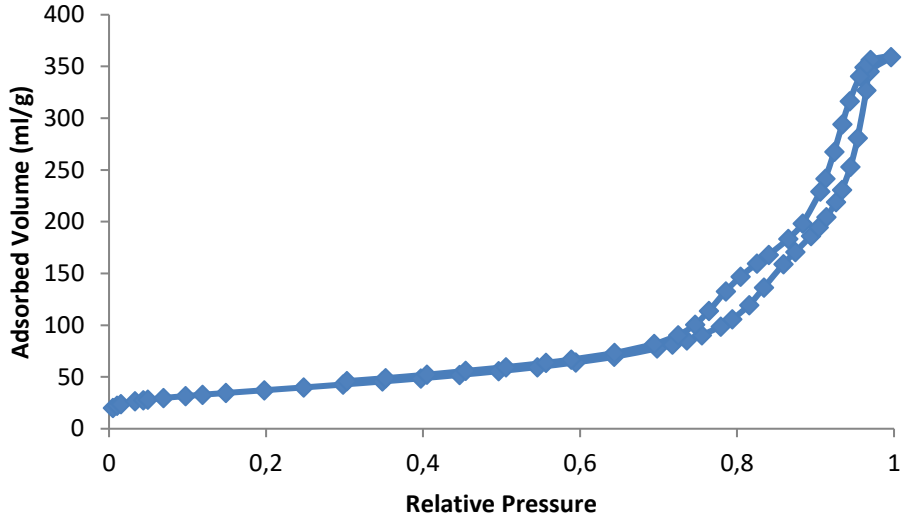

Figure I. 3 - Nitrogen adsorption-desorption isotherm.

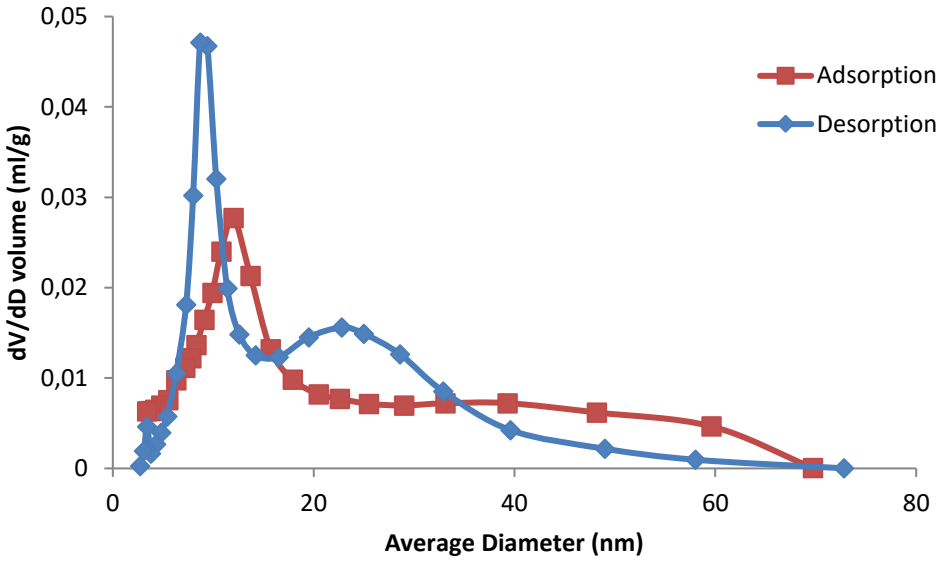

Figure I. 4 - BJH adsorption and desorption.

- For Nickel impregnated with citric acid on HDS catalyst:

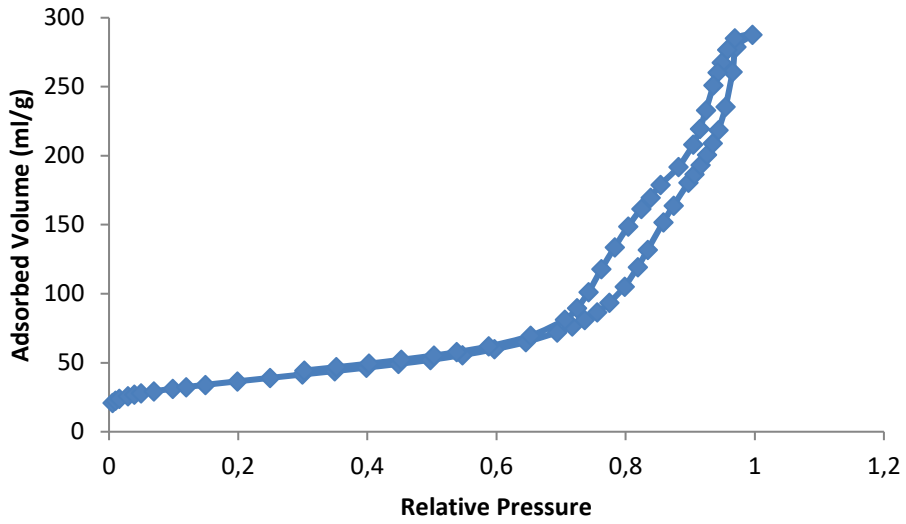

Figure I. 5 - Nitrogen adsorption-desorption isotherm.

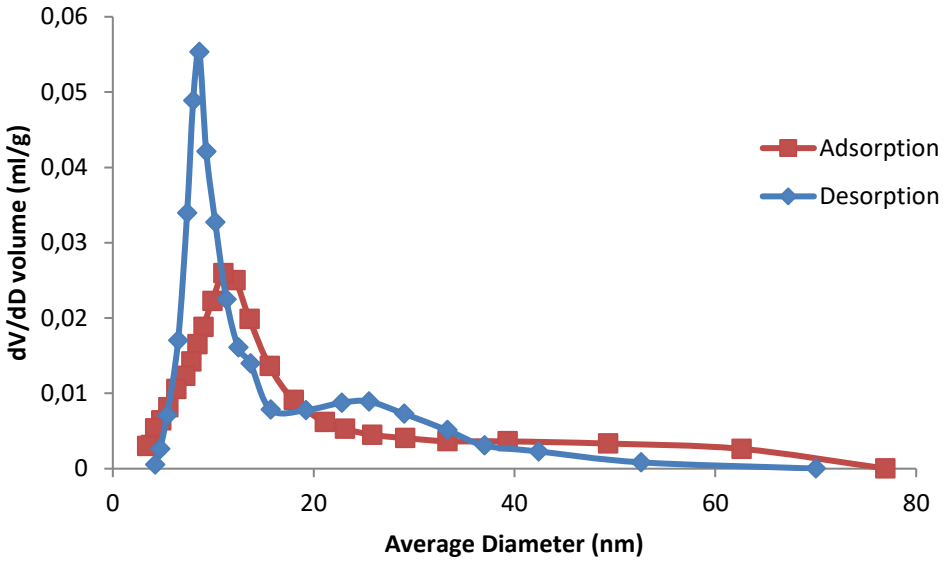

Figure I. 6 - BJH adsorption and desorption.

Results for metals supported on HDS catalyst:

Table I. 1 - Nitrogen adsorption-desorption results.

Catalysts	S_{BET} (m^2/g)	Total porous volume (cm^3/g)
HDS w/ Nickel⁺	132±6.6	0.445±0.009
HDS w/ Copper⁺	117±5.9	0.472±0.009
HDS w/ Cobalt⁺	123±6.2	0.478±0.010
HDS w/ Iron⁺	144±7.2	0.451±0.009

+ prepared with an aqueous solution with citric acid

Mercury porosimetry

Results for metals supported on HDS catalyst:

Table I. 2 - Important results from mercury porosimetry.

Catalysts	Pore Volume for diameter < 7 µm (cm^3/g)	Pore diameter at max dV/dD (nm)	Macropore volume (cm^3/g)	Mesopore volume (cm^3/g)
HDS w/ Nickel⁺	0.79±0.02	12.8	0.33±0.03	0.44±0.02
HDS w/ Copper⁺	0.82±0.02	18	0.36±0.04	0.44±0.02
HDS w/ Cobalt⁺	0.81±0.02	15.2	0.35±0.04	0.44±0.02
HDS w/ Iron⁺	0.76±0.02	9.2	0.32±0.03	0.44±0.02

+ prepared with an aqueous solution with citric acid

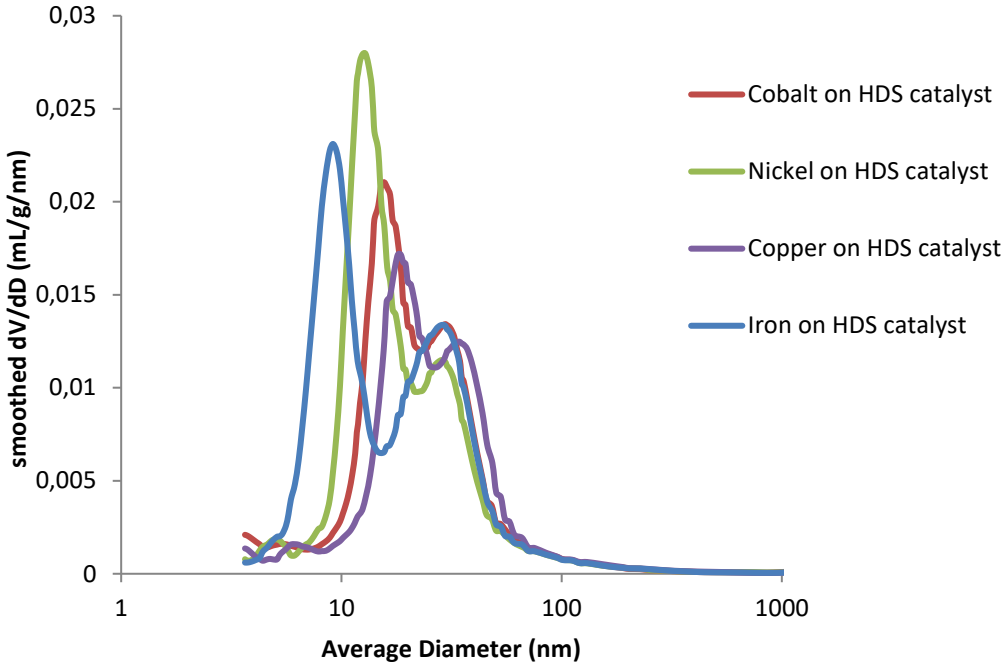

Figure I. 7 – Mercury intrusion.

The pores of the catalysts can be considered as mesopores (3,5-50nm).

X-Ray Difracction

- Metals impregnated on alumina:

For **Cobalt**:

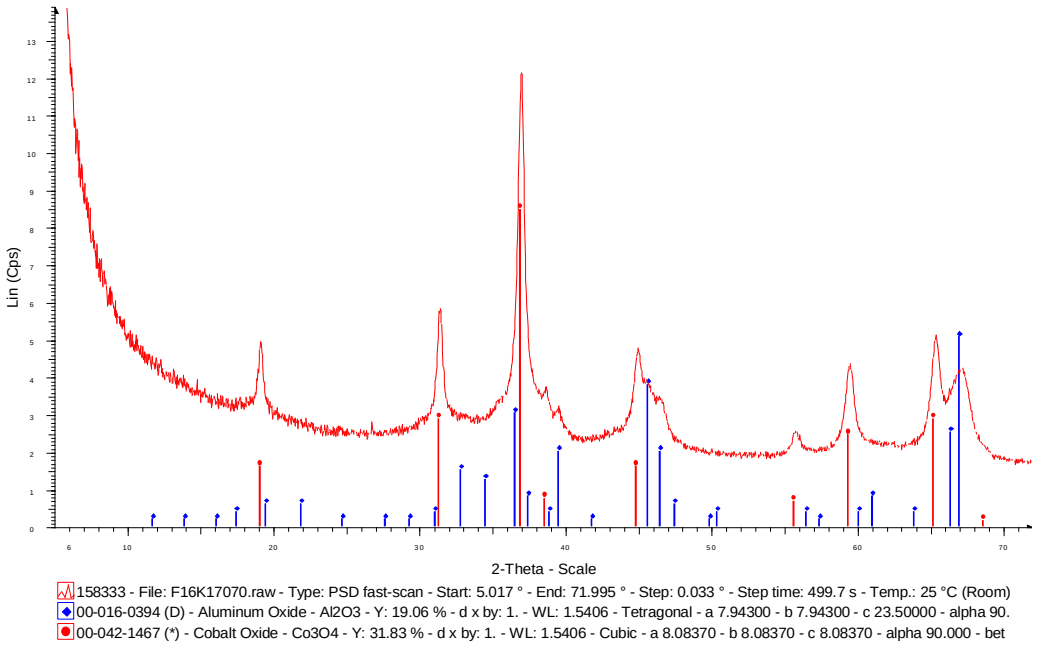

Figure I. 8 - XRD results for cobalt oxide on alumina.

Presence of Co_3O_4 with a measured angle for determine the crystal size of 36.9° (2θ). The crystal size obtained was 175±18 Å.

For **Zinc**:

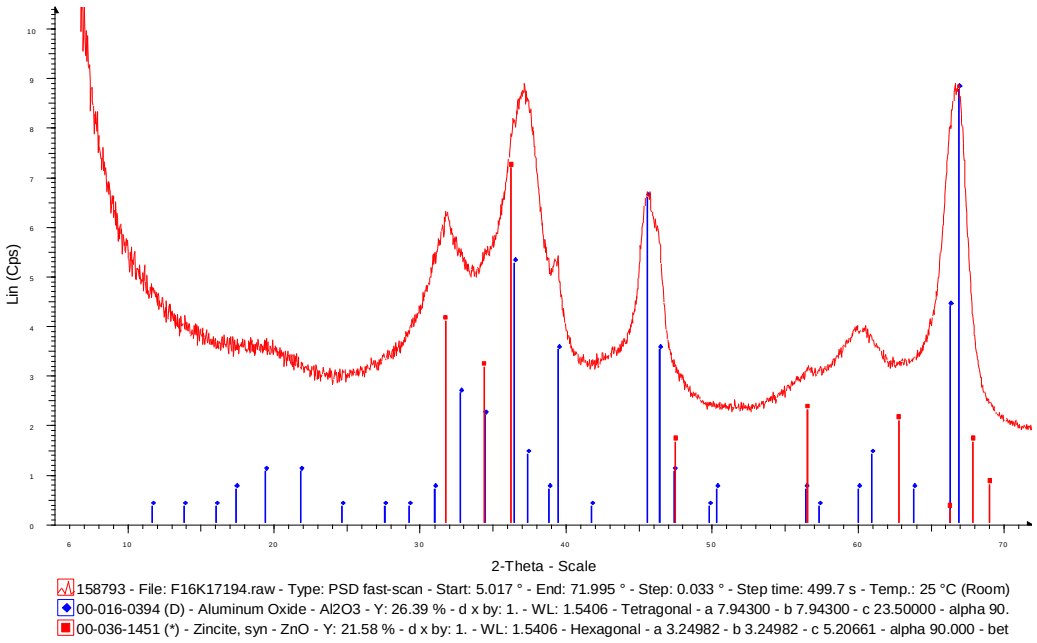

Figure I. 9 - XRD results for zinc oxide on alumina.

Presence of ZnO in a small quantity, impossible to measure the size of the crystal.

For **Copper**:

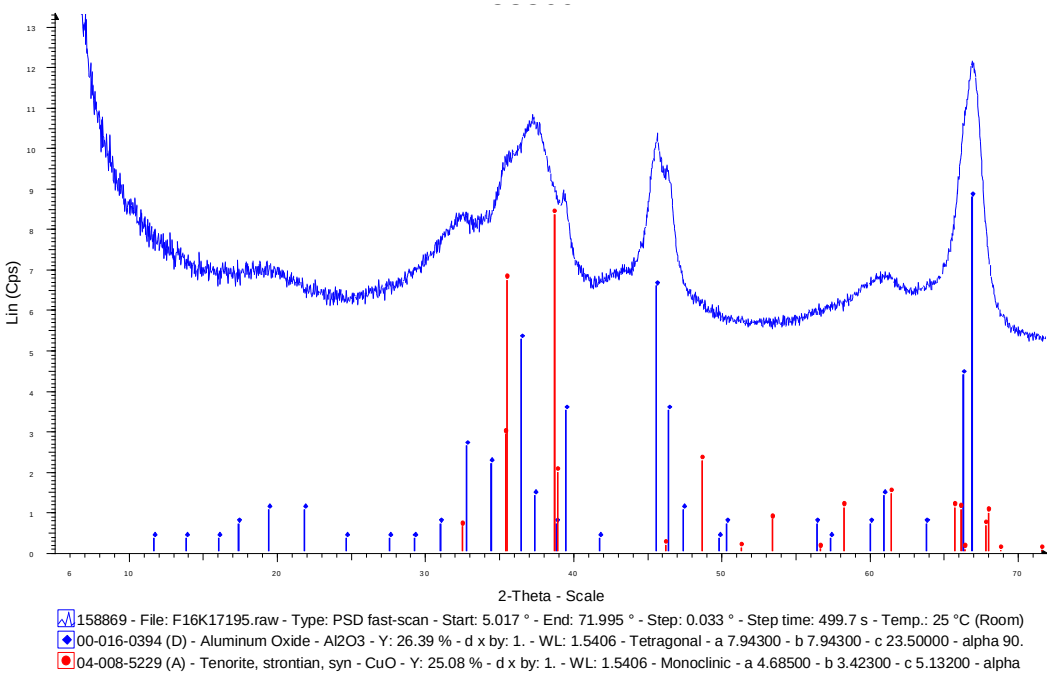

Figure I. 10 - XRD results for copper oxide on alumina.

Presence of CuO in a small quantity, impossible to measure the size of the crystal.

For **Nickel**:

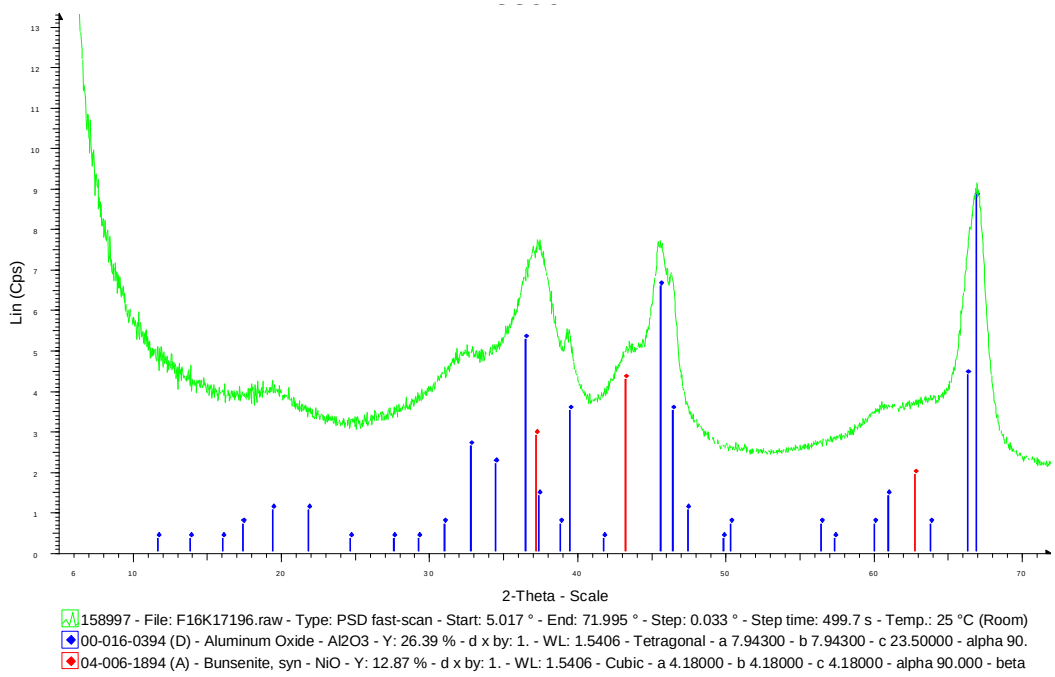

Figure I. 11 - XRD results for nickel oxide on alumina.

Presence of NiO in a small quantity, impossible to measure the size of the crystal.

- Metals impregnated with citric acid on HDS catalyst:

For **Nickel**:

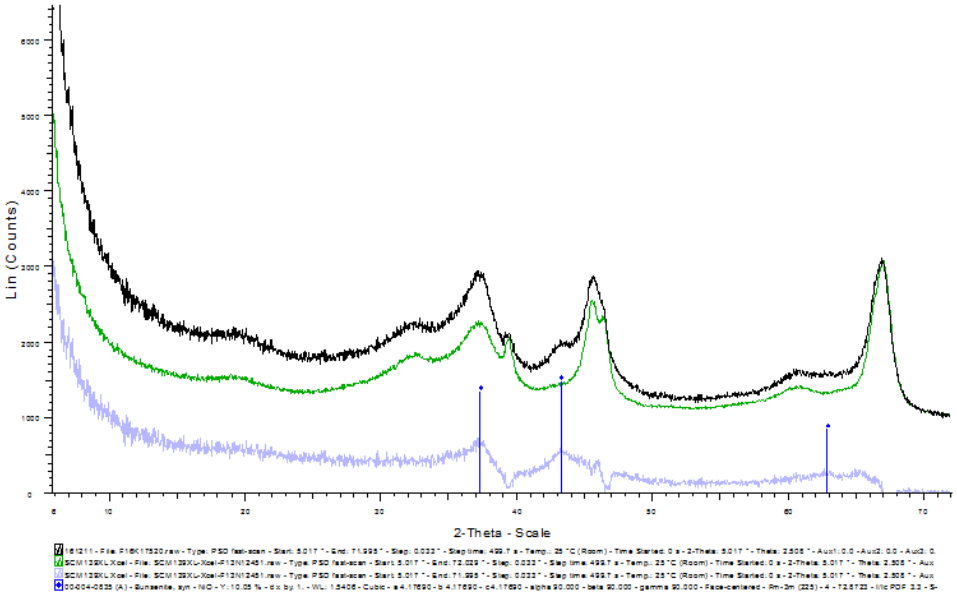

Figure I. 12 - XRD results for nickel oxide on alumina prepared with citric acid.

Presence of NiO with a measured angle for determine the crystal size of 43° (2θ). The crystal size obtained was 30±5 Å.

For **Copper**:

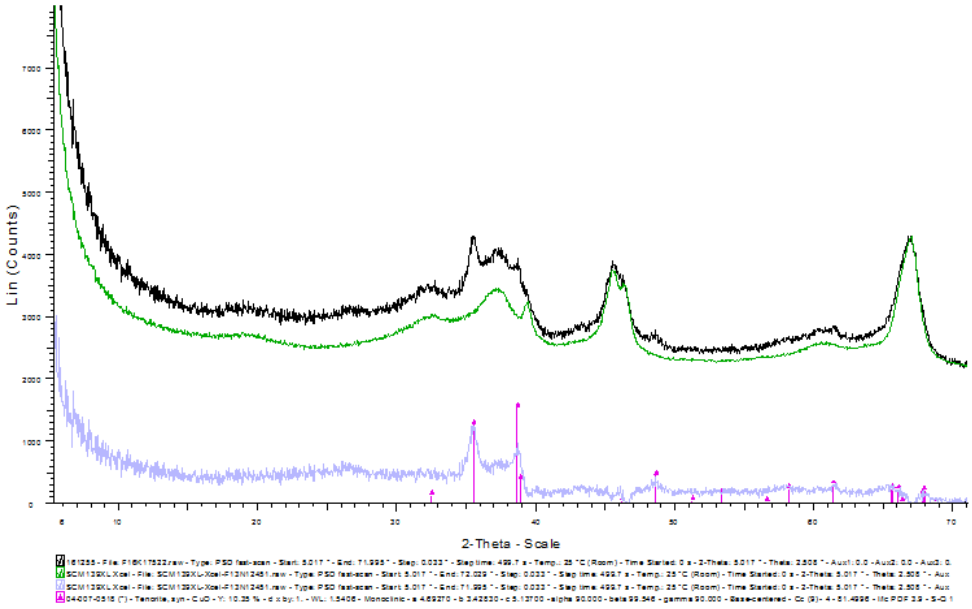

Figure I. 13 - XRD results for copper oxide on alumina prepared with citric acid.

Presence of CuO with a measured angle for determine the crystal size of 48° (2θ). The crystal size obtained was 120±20 Å.

For **Cobalt**:

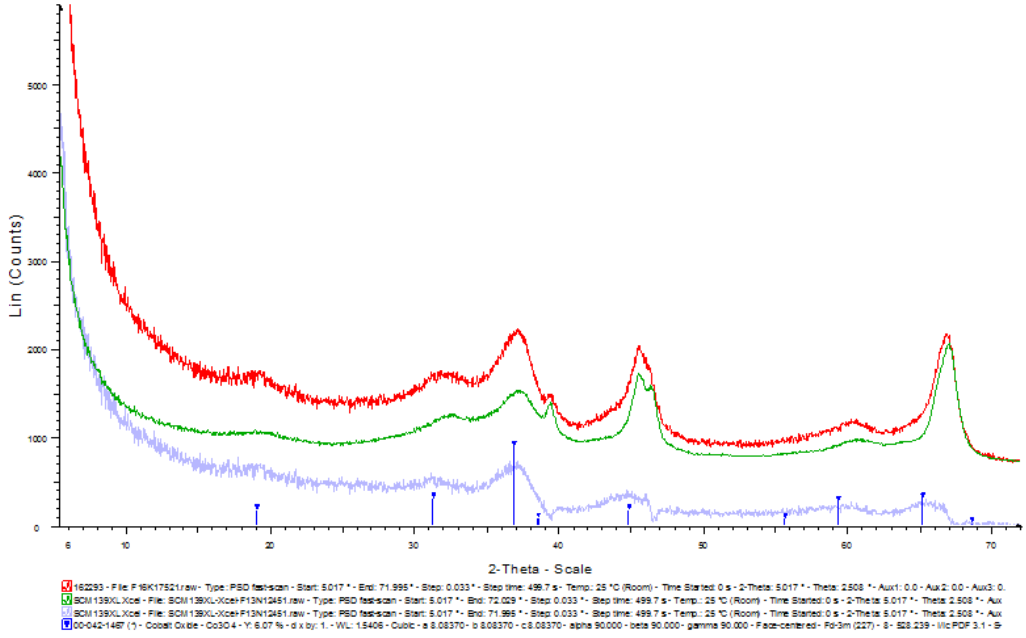

Figure I. 14 - XRD results for cobalt oxide on alumina prepared with citric acid.

Presence of Co_3O_4 with a measured angle for determine the crystal size of 37° (2θ). The crystal size obtained was 30±5 Å.

Remark: For the catalysts impregnated with iron was impossible to determine the crystal size due to an unknown signal.

X-Ray Fluorescence

Results for metals supported on HDS catalyst:

Table I. 3 - Metal contents obtained by X-Ray Fluorescence.

Catalysts	Impregnated metal (wt. %)	Co (wt. %)	Mo (wt. %)
HDS w/ Nickel⁺	7.36±0.26	2.06±0.11	5.71±0.22
HDS w/ Copper⁺	7.37±0.38	2.08±0.11	5.76±0.22
HDS w/ Cobalt⁺	6.91±0.31	8.97±0.31	5.93±0.22
HDS w/ Iron⁺	6.01±0.19	2.10±0.11	5.86±0.22

+ prepared with an aqueous solution with citric acid

Appendix II – Gas Chromatography results

Two examples are given for **RC1** at **t=0; 20; 60; 120min**:

Dearsenification reaction of $AsPh_3$ (215.5ppm As)

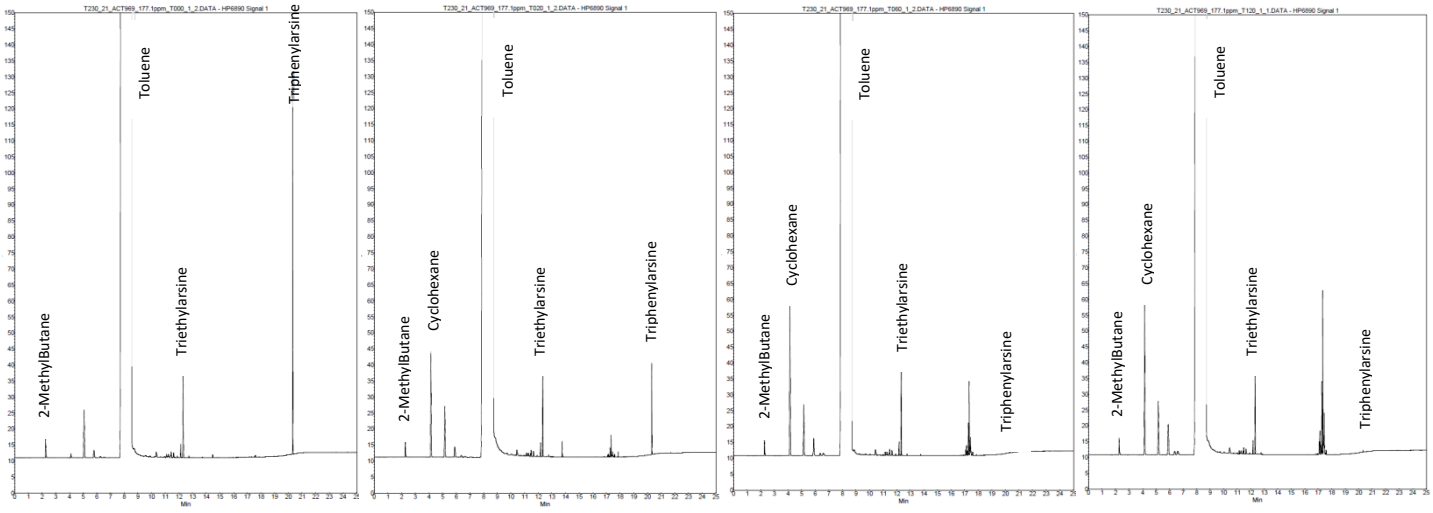

Figure II. 1 – Gas Chromatography results for dearsenification of $AsPh_3$.

It is possible to verify the decrease in the triphenylarsine area with time, followed by the increase in the cyclohexane area (due to the decomposition of triphenylarsine). There are some impurities such as 2-methylbutane and triethylarsine.

Dearsenification and desulfurization reactions with $AsPh_3$ (215.5ppm As, 1000ppm S)

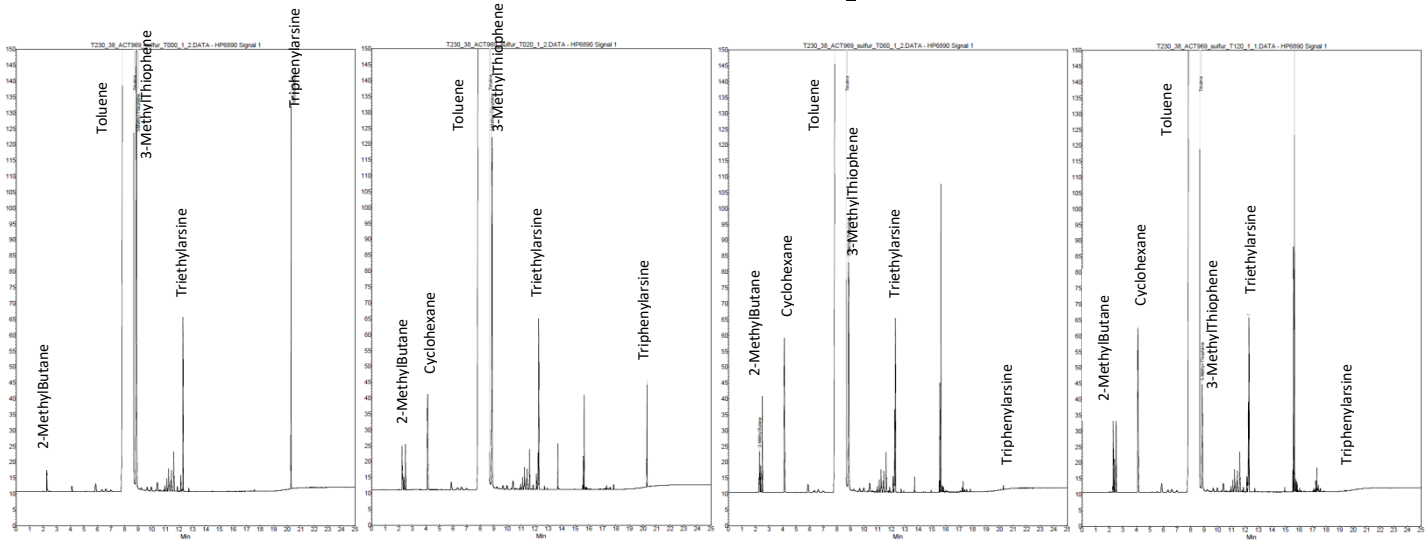

Figure II. 2 – Gas Chromatography results for dearsenification and desulfurization with $AsPh_3$.

It is possible to verify the decrease in the triphenylarsine and 3-methylthiophene areas with time, followed by the increase in the cyclohexane (due to the decomposition of triphenylarsine) and 2-methylbutane area (due to the hydrogenation of 3-methylthiophene). There are some impurities such as triethylarsine.